Reply to Anonymous Referee #1's comments

Dear referee,

We appreciate your careful review and comments on this manuscript. We took your all comments into consideration as follows. Our replies to your main comments (MC) are listed below, followed by replies to your detailed comments (DC) in the annotated pdf.

Sincerely,
Hanaya Okuda, Ikuo Katayama, Hiroshi Sakuma, Kenji Kawai

MC 1

This manuscript reports a series of experiments on brucite at various normal stress conditions and uses the results of these experiments to make inferences on the nucleation of slow earthquakes. Specifically, the authors find a low coefficient of friction, which, together with negative values of the rate and state friction parameter (a-b) is used to claim that brucite is a key material controlling the nucleation of slow earthquakes in hydrated mantle wedges.
The data in this manuscript is of interest to the community working on fault frictional behaviour and deserves to be published. However, the manuscript needs to be improved significantly before publication. My main comments are listed below and detailed comments are given in the annotated pdf.

1. The context of the current study needs clarification. The Introduction is not written very concisely and the role of mantle wedges in explaining any type of behaviour along subduction zones is not clearly outlined. Why focus on the mantle wedge and not the subduction plate interface? In addition, the authors use the current study to make inferences on slow earthquake nucleation but slow earthquakes are not defined and the reason for attempting to explain them is not clear. I suggest significant revision and rewriting of the manuscript as a whole (see also below) but in particular of the Introduction.

Reply to MC 1

Thank you for the comment. Practically, our study is focused at the site near the plate interface. The hydrated mantle wedge materials, i.e., serpentinite minerals, compose the plate interface between the subducting oceanic crust and the mantle, and the seismic activities in this area are proposed to be controlled by serpentinite (e.g., Guillot et al., 2015; Hirt & Guillot, 2015). Therefore, we used the term "the mantle wedge" in this study. However, "the subduction plate

interface in the mantle wedge" would be more accurate to describe the region of focus in this study. We modified the title as follows:

(Before) Effect of normal stress on the friction of brucite: Application to slow earthquake in the mantle wedge

(After) Effect of normal stress on the frictional behavior of brucite: Application to slow earthquakes at the subduction plate interface in the mantle wedge

Further, we added some sentences and arranged the structure of the Introduction. Serpentinite had been classically considered to be aseismic and to be an explanation for the downdip limit of the seismogenic zone. However, recent seismological observations found slow earthquakes (e.g., ETS, SSE, or LFE) at the subduction plate interface in the mantle wedge. Because slow earthquakes can trigger or be triggered by huge megathrust earthquakes, the nucleation mechanisms of those slow earthquakes are important for understanding the seismic activities at the subduction zones. Previous studies suggested that frictional characteristics of serpentinite may control the nucleation of slow earthquakes; therefore, frictional properties of serpentinite should be better understood. We rewrote the Introduction section to explain this. Please also refer to Comment 6 by referee #2.

MC 2

2. Slow earthquakes in subduction zones have been addressed before via experimental studies. These focus on the subduction interface rather than the mantle wedge, but I feel that they should be mentioned in the Discussion (e.g. Ikari et al., 2013, Nature GeoScience, DOI: 10.1038/NGEO1818; Den Hartog et al, 2012, JSG, DOI:10.1016/j.jsg.2011.12.001).

Reply to MC2

As the referee commented, other possibilities, such as the transition from negative to positive a-b or the slip-weakening behavior may generate slow earthquakes, as indicated by those studies. We added some sentences and references in the Introduction (lines 131–138 in the marked-up manuscript) and Discussion (lines 540–544 in the marked-up manuscript) that explain some of the proposed mechanisms for the occurrence of slow earthquakes.

MC 3

3. The manuscript contains a number of very bold statements which lack appropriate evidence. In particular, the interpretation of the behaviour of brucite gouge as being controlled by boundary shears is not fully justified in my view. Notably, how can the presence of Riedel shears be explained if the boundary shears would control sliding behaviour?

Reply to MC3

Riedel shear developed at the initial stage of the deformation and shortened the gouge width. However, after the peak friction coefficient, the gouge thickness was kept constant, which means that the deformation may occur parallel to the shear displacement. Moreover, we observed a clear alignment of the particle along the boundary shear but no alignment along the Riedel shear, suggesting that the deformation along the Riedel shear was not the dominant process during the steady state. Therefore, the Riedel shears were thought to be not active and just preserved after the yield point. Shear localization along the boundary shear, not along the Riedel shears, was also observed in previous studies (e.g., Haines et al., 2009). Indeed, deformation along the Riedel shear may not be completely inactive, but our microstructural observation suggests that the deformation along the boundary shear is more effective. However, as commented in DC67, we need to clearly state the evidence of the shear localization along the boundary shear. Notably, we think our original manuscript lacked the description of the variation in gouge thickness during the experiment; therefore, we updated the text as follows (line 384–386 in the marked-up manuscript):

> **(Before)** The gouge width remained almost constant following the post-yield and in the steady state.
>
> **(After)** The gouge thickness remained almost constant after the post-yield and steady state, suggesting that the deformation may localize parallel to the shear deformation, i.e., parallel to the boundary shear.

Further, our original manuscript lacked the explanation that we had not observed any alignment along Riedel shears; therefore, we added the following sentence at lines 417–419 in the marked-up manuscript:

> We did not observe any alignment along the Riedel shears, suggesting that deformation along the Riedel shears cannot be dominant at the steady state.

MC 4

4. The writing style and English of the manuscript should be revised and improved. Please see the annotated pdf for examples.

Reply to MC4

We are sorry for our poor writing and appreciate your grammatical corrections on the manuscript. We have now used an English correction service to improve the manuscript.

DC 1 in line 1

"frictional behaviour" or "friction coefficient" would be better

Reply to DC1

We modified the title as follows:

(Before) Effect of normal stress on the friction of brucite: Application to slow earthquake in the mantle wedge

(After) Effect of normal stress on the frictional behavior of brucite: Application to slow earthquakes at the subduction plate interface in the mantle wedge

DC 2 in line 2

Insert "s".

Reply to DC2

Per this comment, we modified the title as shown in the reply to DC1.

DC 3 in line 22

Replace "The microstructural observations" into "Microstructural observations".

Reply to DC3

Per this comment, we removed "The" from the text (line 24 in the marked-up manuscript).

DC 4 in line 23

Replace "the" into "a".

Reply to DC4

Per this comment, we modified the article (line 25 in the marked-up manuscript).

DC5 in lines 25-27

This is confusing. It suggests that other minerals are considered, but these are not mentioned. This statement misses context.

Reply to DC5

We have reviewed the frictional characteristics of other serpentinite minerals in the Discussion; therefore, we modified the text (lines 26–28 in the marked-up manuscript) as follows:

(Before) Brucite is found to be the only mineral that has a low friction coefficient and exhibits unstable frictional behavior under hydrated mantle wedge conditions, explaining the occurrence of slow earthquakes in the mantle wedge.

(After) Among serpentinite-related minerals, weak and unstable frictional behavior of brucite under the hydrated mantle wedge conditions may play a role in slow earthquakes at the subduction plate interface in the mantle wedge.

DC6 in line 36

Remove "due".

Reply to DC6

Per this comment, we removed "due" (line 40 in the marked-up manuscript).

DC7 in lines 42-44

This needs some clarification. Presumably, a different mineral composition of serpentinite means that the related mineral will have a different composition (to have the same overall chemical make up)?

Reply to DC7

Mineral compositions of serpentinite vary depending on pressure and temperature conditions. In this sentence, we would like to explain that because each mineral has a different frictional characteristic, it is important to consider frictional properties of all serpentinite-related minerals in order to understand the frictional behavior of bulk serpentinite. To make it clear, we modified this sentence (lines 86–89 in the marked-up manuscript) as follows:

(Before) The mineral composition of serpentinite has a strong effect on the mechanical behavior of bulk serpentinite because each serpentinite-related mineral, such as antigorite, brucite, and talc, has a different frictional behavior.

(After) Serpentinite is made up of serpentinite-related minerals, such as antigorite, brucite, and talc, and as those minerals show different frictional behavior, the frictional properties of each mineral should be understood to interpret the mechanical behavior of bulk serpentinite.

DC8 in line 48

Remove "compared with other serpentinite-related minerals."

Reply to DC8

Per this comment, we removed this part from the sentence. In addition, we separated this sentence into two parts according to referee #2 Comment 2 (lines 89–93 in the marked-up manuscript).

(Before) Despite a variety of previous experimental investigations of the frictional properties of antigorite and talc (Hirauchi et al., 2013; Moore et al., 1997; Moore and

Lockner, 2007, 2008; Okazaki and Katayama, 2015; Reinen et al., 1994; Sánchez-Roa et al., 2017; Takahashi et al., 2007; Tesei et al., 2018), brucite has rarely been considered in previous studies compared with other serpentinite-related minerals, which might be due to the fact that it is difficult to detect brucite under natural conditions because of its fine-grained nature (Hostetler et al., 1966).

(After) Many previous experimental studies investigated the frictional properties of antigorite and talc (Hirauchi et al., 2013; Moore et al., 1997; Moore and Lockner, 2007, 2008; Okazaki and Katayama, 2015; Reinen et al., 1994; Sánchez-Roa et al., 2017; Takahashi et al., 2007; Tesei et al., 2018). However, brucite has rarely been considered in previous studies, as it is challenging to detect brucite under natural conditions because of its fine-grained nature (Hostetler et al., 1966).

DC9 in lines 50-51

Please clarify why this is and the relevance of this.

Reply to DC9

We understand that the metasomatic reaction between serpentinite and meta-sedimentary rock occurs at the subduction plate interface as observed in geological studies. Deformation within such a metasomatic layer was observed (e.g., Tarling et al., 2019) and reacted minerals like talc are weak and deform easily (e.g., Hirauchi et al., 2013); therefore, the Si metamorphism does affect on the deformation property of serpentinite layer at the interface. However, the metamorphic layer is often narrow, and Si is effectively consumed according to both geological and hydrothermal experiments (e.g., Kawahara et al., 2016; Mizukami et al., 2014; Oyanagi et al., 2015, 2020). Therefore, we expect that the serpentinite layer, which is often several hundred of meters to kilometers wide, possibly contains brucite. Practically, brucite was found from shallow mantle wedge conditions (e.g., Kawahara et al., 2016; Mizukami et al., 2014). Indeed, we have to assess the frictional properties of metamorphic zones like talc within the serpentinite layer to understand the deformation at the subduction plate interface. But we still need to understand the deformation properties of the matrix part of serpentinite layer, which may contain brucite. We added some sentences, in lines 99–113 in the marked-up manuscript, to describe them.

DC10 in line 59

Replace "stick-slip behavior is significant" into "significant stick-slip behavior has been observed."

Reply to DC10

Per this comment, we modified this sentence (lines 123–124 in the marked-up manuscript).

DC11 in line 60

Insert "behavior."

Reply to DC11

Per this comment, we inserted "behavior" (line 125 in the marked-up manuscript).

DC12 in line 62

Replace "the" into "a."

Reply to DC12

Per this comment, we replaced the article (line 127 in the marked-up manuscript).

DC13 in lines 70-71

This seems too much generalized. Please underpin this strong statement with evidence.

Reply to DC13

Per this comment, we modified the text (lines 68–79 in the marked-up manuscript) as follows:

(Before) The effective normal stress is an important parameter that constrains the frictional behavior because the apparent frictional strength of a material decreases with decreasing effective normal stress. Near lithostatic pore pressure conditions, which lead to low effective normal stress conditions, have been inferred based on seismic velocity structures at the plate interfaces of several subduction zones where slow earthquakes coincidentally occur such as Cascadia, SW Japan, Central Mexico, and Hikurangi (Audet et al., 2009; Audet and Kim, 2016; Eberhart-Phillips and Reyners, 2012; Matsubara et al., 2009; Shelly et al., 2006; Song and Kim, 2012). Importantly, low effective normal stress seems favorable for the nucleation of slow earthquakes (Liu and Rice, 2007, 2009; Rubin, 2008; Segall et al., 2010).

(After) In addition, near lithostatic pore pressure conditions, which lead to low effective normal stress conditions, have been inferred based on seismic velocity structures at the plate interfaces of several subduction zones where slow earthquakes coincidently occur in the regions such as Cascadia, SW Japan, Central Mexico, and Hikurangi (Audet et al., 2009; Audet and Kim, 2016; Eberhart-Phillips and Reyners, 2012; Matsubara et al., 2009; Shelly et al., 2006; Song and Kim, 2012). This low effective normal stress condition may be correlated to the occurrence of slow earthquakes because frictional deformation becomes dominant, rather than viscous deformation, in terms of shear strength (French and Condit, 2019; Gao and Wang, 2017). Furthermore, the low effective normal stress condition seems

favorable for the nucleation of slow earthquakes (Liu and Rice, 2007, 2009; Rubin, 2008; Segall et al., 2010) and is also consistent with smaller stress drops than regular earthquakes (Ide et al., 2007; Rubinstein et al., 2007, 2008; Schmidt and Gao, 2010). Thus, frictional properties of serpentinite under the low effective normal stress condition likely play an important role in the occurrence of slow earthquakes at the subduction plate interface near the mantle wedge.

Please note that these sentences were moved to the third paragraph according to comment 7 from referee #2.

DC14 in line 72

Remove "s."

Reply to DC14

Per this comment, we removed "s" (line 68 in the marked-up manuscript)

DC15 in line 76

This is probably a too strong statement. "seems" would be better here.

Reply to DC15

Per this comment, we modified "is" into "seems" (line 75 in the marked-up manuscript)

DC16 in line 78

Insert "s."

Reply to DC16

This sentence was removed during the revision.

DC17 in line 83

Remove "a."

Reply to DC17

Per this comment, we removed this sentence according to DC18 (please see below).

DC18 in lines 83-85

This is only true if fault motion localizes in brucite-rich layers, which I think would be very speculative.

Reply to DC18

Based on previous geological studies on the paleo-mantle wedge that showed brucite can stably exist in serpentinite, we think that brucite is one of the important phases controlling frictional behavior at the subduction plate interface in the hydrated mantle wedge. Moreover, based on our microstructural observations, we noted that a small volume of brucite can weaken the serpentinite bulk strength. According to the information above, we think that the weak, unstable frictional behavior of brucite may play a key role in the nucleation of slow earthquakes. In the Introduction, however, readers cannot access enough information to reach this conclusion; therefore, we removed this sentence from the manuscript.

DC19 in line 96

Insert "s."

Reply to DC19

Per this comment, we inserted "s" (line 175 in the marked-up manuscript)

DC20 in lines 98-99

In my understanding, the brucite is the gouge, so please reformulate.

Reply to DC20

Per this comment, we modified the text (lines 178–179 in the marked-up manuscript) to make it clear as follows:

(Before) the brucite powder was quickly placed in each of the two gouges

(After) the brucite powder was quickly sandwiched between the blocks to form the gouge

DC21 in line 109

I do not think that you can call this saturated as no vacuum was applied so the gouge likely still contained some air. "Water-wet" would be more accurate.

Reply to DC21

Per this comment, we replaced "water-saturated" with "water-wet" (line 190 in the marked-up manuscript)

DC22 in line 116 (Figure 1)

The "Stainless spacer" should probably be "Stainless steel spacer".

Reply to DC22

Per this comment, we corrected it to “stainless steel spacer.” Please refer to the comment below.

DC23 in line 118 (Figure 1)

The text in this figure is very small and hard to read (this includes the scale bar in a). I would suggest increasing the size of the text.

Reply to DC23

Per this comment, we modified Figure 1 as follows:

(Before)

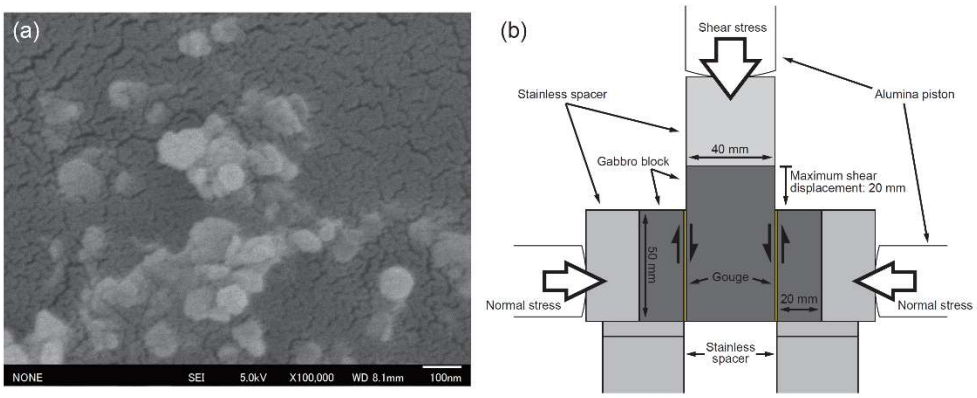

(After)

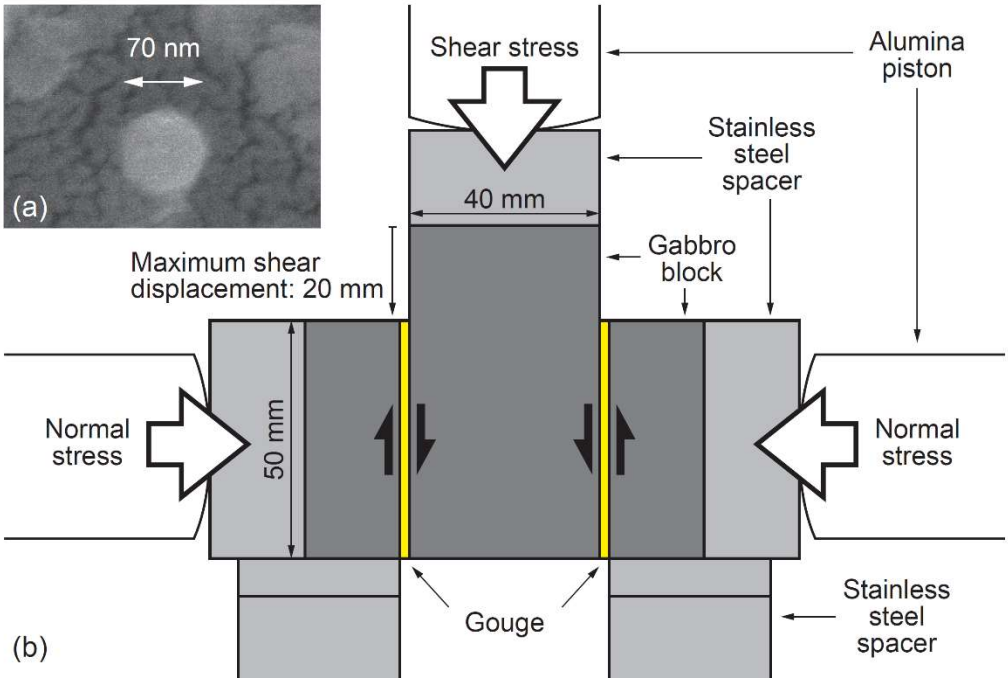

DC24 in line 126

The cohesion should be compared to the shear strength of the samples, not the normal stress.

Reply to DC24

We modified the sentence (lines 208–210 in the marked-up manuscript) as follows:

(Before) Note that cohesion was not considered because the cohesion stresses were 0.36 and 0.47 MPa for the dry and wet cases, respectively, which are much smaller than the tested normal stress conditions.

(After) Note that cohesion stresses were 0.36 and 0.47 MPa for dry and wet cases, respectively, calculated by linear regression of shear stress and normal stress of all the experiments. Because the obtained cohesion stresses were too small to affect the friction coefficients, the cohesion stress was not considered in this study.

DC25 in lines 129-130

This sentence needs rewriting and clarification:

- "the latter part of each velocity step" needs to be clarified.

- "detrending" a "slip dependency" (grammar of the sentence) is incorrect and needs correction.

- "The slip dependency" needs clarification itself.

Reply to DC25

We rewrote the sentence (lines 215–217 in the marked-up manuscript) as follows:

(Before) The slip dependency, which was calculated from the later part of each velocity step test with a shear displacement of 500 μm, was detrended before conducting the following analyses.

(After) Before conducting the following analyses, the friction coefficient versus the displacement curve was detrended for the slip-weakening trend, which was obtained from the friction data in the second half of each velocity step of 500 μm shear displacement.

DC26 in line 135

Please clarify what is meant here.

Reply to DC26

We modified the text (lines 223–224 in the marked-up manuscript) as follows:

(Before) The transition of V was calculated by the following relationship:

(After) We estimated the effect of elastic interaction due to the machine stiffness on V using the following relationship:

DC27 in line 148-149

Pleases clarify "downsteps" and "upsteps".

Reply to DC27

We modified the text (lines 237–239 in the marked-up manuscript) as follows:

(Before) Note that d_c for the downsteps is larger than that for the upsteps.

(After) Note that d_c values for the velocity steps whose velocities decreased from 33 to 3 μm s^{-1} (downsteps) are larger than those for the velocity steps whose velocities increased from 3 to 33 μm s^{-1} (upsteps).

DC28 in line 150

Please clarify.

Reply to DC28

To make the word "asperity contact" clear, we modified the text (lines 240–241 in the marked-up manuscript) as follows:

(Before) d_c reflects the contact diameter of the asperity contact

(After) d_c reflects the diameter of the contact area between grains

DC29 in line 151

Replace "becomes" into "is."

Reply to DC29

Per this comment, we modified it (line 243 in the marked-up manuscript).

DC30 in line 152

Replace "becomes" into "is."

Reply to DC30

Per this comment, we modified it (line 244 in the marked-up manuscript).

DC31 in lines153-154

Please clarify. Presumably you are referring here to solving for a and b separately vs. for a-b?

Reply to DC31

We calculated a and b separately at first, then obtained $a-b$ from the calculated a and b. To describe this more clearly, we modified the text (244–252 in the marked-up manuscript) as follows:

(Before) Although there are still debates on the choice of constitutive laws (Bhattacharya et al., 2015, 2017; Marone, 1998), the value of $a-b$ is more critical for seismic activities.

(After) Although there are still debates on the choice of constitutive laws (Bhattacharya et al., 2015, 2017; Marone, 1998), as all constitutive laws give the same result on $a-b$, we calculated the value of $a-b$ by using separately obtained a and b with the aging law. The focus of this study will be the $a-b$ value because it plays an essential role in the nucleation process of earthquakes. However, other parameters like d_c and stiffness are also important to the nucleation process, and therefore, those parameters should be assessed in future studies.

Please note that this modification includes Comment 14 by the referee #2.

DC32 in line 156

Replace "the" into "a."

Reply to DC32

Per this comment, we modified the article (line 256 in the marked-up manuscript).

DC33 in line 157

Replace "the" into "a."

Reply to DC33

Per this comment, we modified the article (line 257 in the marked-up manuscript).

DC34 in line 165 (about chapter 2.2.2)

The fact that brucite is a sheet-structure mineral should be mentioned in the Introduction.

Reply to DC34

Per this comment, we added the sentence which explains that brucite is a sheet-structure mineral in lines 116–118 in the marked-up manuscript as follows:

Furthermore, as brucite is a sheet-structure mineral, which often shows a low friction coefficient due to weak interlayer bonding, its frictional behavior may play a role in earthquakes at the serpentinite layer (Moore et al., 2001; Moore and Lockner, 2004).

DC35 in line 167

Please correct. Do you mean "composed of"?

Reply to DC35

Per this comment, we corrected it to “composed of” (line 273 in the marked-up manuscript).

DC36 in line 169

Insert “the.”

Reply to DC36

Per this comment, we inserted “the” (line 275 in the marked-up manuscript).

DC37 in line 170

Remove “the.”

Reply to DC37

Per this comment, we removed it (line 275 in the marked-up manuscript).

DC38 in line 170

Insert “s.”

Reply to DC38

Per this comment, we inserted “s” (line 275 in the marked-up manuscript).

DC39 in lines 170-173

Please be explicit what is meant here.

Reply to DC39

The sentence “Under natural conditions, the aligned platy particles of interconnected talc were reported to contribute to the low friction coefficient of low angle normal faults (Collettini et al., 2009).” represents the importance of the crystal orientation of platy particles within the gouge. What we wanted to express in the sentence “The experimentally determined friction coefficients of single-crystalline muscovite and chlorite are much smaller than those of powdered polycrystalline samples (Horn and Deere, 1962; Kawai et al., 2015; Niemeijer, 2018; Okamoto et al., 2019).” was that the alignment of sheet-structure minerals has a significant effect on frictional strength. However, those studies mainly compared single-crystalline and powdered

polycrystalline sheet-structure minerals. Therefore, considering the next comment, we removed the sentence from the manuscript because those references do not directly show the effect of the alignment of sheet-structure minerals on friction.

DC40 in lines 173-174

This conclusion does not follow from the foregoing text.

Reply to DC40

As we modified the texts in reply to DC39, we think the problem is now solved. Please see the above.

DC41 in line 176

Remove "s."

Reply to DC41

Per this comment, we removed "s" (line 282 in the marked-up manuscript).

DC42 in lines 176-177

Please add some details on how these were prepared.

Reply to DC42

To explain the procedures for the preparation of thin sections, we modified the text (lines 282–285 in the marked-up manuscript) as follows:

(Before) Thin sections parallel to the shear direction and normal to the gouges with a thickness of 30 μm were prepared.

(After) After the experiment, we impregnated the gouge and the blocks with epoxy resin to keep the deformation structures within the gouge. Thin sections parallel to the shear direction and normal to the gouges with a thickness of 30 μm were prepared from the impregnated samples.

DC43 in lines 186-187

Please be more specific in this definition of the peak friction coefficient - "initially" is too vague and would best be replaced by a quantification of the displacement range.

Reply to DC43

We added the quantitative description of the displacement for the peak friction coefficient (lines

294–295 in the marked-up manuscript) as follows:

(Before) In general, both dry and wet experiments initially show high friction coefficients

(After) In general, both dry and wet experiments show high friction coefficients at a shear displacement of 1.5–2 mm

DC44 in line 187

Replace "lasting about 10 mm shear displacement" into "with a shear displacement of about 10 mm."

Reply to DC44

Per this comment, we replaced the text (line 296 in the marked-up manuscript).

DC45 in line 187

Insert "s."

Reply to DC45

Per this comment, we inserted "s" (line 296 in the marked-up manuscript).

DC46 in line 188

Remove "the."

Reply to DC46

Per this comment, we removed it (line 297 in the marked-up manuscript).

DC47 in line 188 (about the description of "steady state")

It does not seem like a true steady state is reached, so it would be better to use the term "final friction coefficients" rather than "steady state" friction coefficients.

Reply to DC47

According to the comment we modified the description of "steady state friction coefficient" into "final friction coefficient." In the microstructural analyses, we still use the term "steady state" because the microstructure of the gouge at the 10 mm shear displacement is consistent with the microstructure at the "steady state," and the friction coefficient and gouge thickness were almost constant. We added some sentences in lines 370–373 in the marked-up manuscript as follows:

> Note that the steady state may not be achieved at a shear displacement of 10 mm, but as the final friction coefficients were similar to the friction coefficients at 10 mm shear displacement, here we used the term "steady state" and considered that the microstructure

at 10 mm shear displacement might be consistent with the steady state.

DC48 in line 189

What are the numbers between brackets? This is confusing. If it is extra precision - please decide on only one level of precision for reporting.

Reply to DC48

The brackets meant the standard deviation of multiple experiments. To avoid confusion, we fixed the descriptions as follows:

(Before) 0.40(4) and 0.26(3)

(After) 0.40±0.04 and 0.26±0.03

We also modified other parts, including Table 1.

DC49 in line 193

Insert "s."

Reply to DC49

Per this comment, we inserted "s" (line 302 in the marked-up manuscript)

DC50 in line 206 (Figure 3)

"Previous" contains a typo

Reply to DC50

We are sorry for the typo; we corrected it.

DC51 in line 210 (Caption for Figure 3)

Replace "insignificantly depend on" into "do not show a clear trend with normal stress."

Reply to DC51

Per this comment, we corrected it (line 318 in the marked-up manuscript).

DC52 in lines 213-214 (Caption for Figure 3)

This looks like an experimental artifact rather than the inherent frictional behaviour of brucite. How reliable is this data?

Reply to DC52

We do not exactly understand what caused this sudden stress drop; therefore, we did not discuss the peak value of wet brucite for 60 MPa normal stress. To make this point clear, we added the sentence in the figure caption as follows:

(Before) Note that the peak friction coefficient of wet brucite at an effective normal stress of 60 MPa is high because of sudden stress drops in the initial stage of the shear displacement (Fig. S1).

(After) Note that the peak friction coefficient of wet brucite at an effective normal stress of 60 MPa is high because of sudden stress drops in the initial stage of the shear displacement (Fig. S1). As this data may include some experimental artifacts, we do not use this peak value in this study.

We also added the sentence in the main text in lines 303–306 in the marked-up manuscript as follows:

(Before) Note that the peak friction coefficient of wet brucite at an effective normal stress of 60 MPa is high because of sudden stress drops in the initial stage of the shear displacement (Fig. S1).

(After) Note that the peak friction coefficient of wet brucite at an effective normal stress of 60 MPa is high because of sudden stress drops in the initial stage of the shear displacement (Fig. S1). As this data may include some experimental artifacts, we do not use this peak value for 60 MPa normal stress in this study.

DC53 in lines 222-223

I suggest leaving this out as the current experiments do not give information on effects of numerous other variables, such as temperature, grain size, etc.

Reply to DC53

We agree with the referee. Per this comment and Comment 15 by referee #2, we deleted the sentence and just stated that the $a-b$ values do not differ between upsteps and downsteps (lines 329–331 in the marked-up manuscript) as follows:

(Before) The $a-b$ values obtained for the upsteps and downsteps insignificantly differ (Figs. 4a and b), which implies that the normal stress condition mainly controls the $a-b$ values.

(After) The $a-b$ values obtained for the upsteps and downsteps insignificantly differ (Figs. 4a and b).

DC54 in lines 223-224

Please be more accurate in this description - this is not quite what can be seen in Figure 4.

Reply to DC54

To describe the results more in detail, we modified the sentence (lines 333–337 in the marked-up manuscript) as follows:

(Before) The constitutive parameter a insignificantly depends on the applied normal stress, whereas b decreases as the normal stress increases, leading to the transition from negative to positive $a-b$ values (Figs. 4e and f).

(After) In the experiments with normal stress conditions of 20, 40, and 60 MPa, the constitutive parameter a is almost constant with 0.0054 for both upsteps and downsteps, whereas b decreases from 0.0064 to 0.0042 and from 0.0076 to 0.0040 for upsteps and downsteps, respectively, as the normal stress increases (Figs. 4e and f). Accordingly, we concluded that the decrease in b induces the transition from negative to positive $a-b$.

DC55 in lines 228-229

Presumably, (a-b) was not determined for experiments that showed stick-slip. Please mention this explicitly (according to Figure 4 this should be stated in the text). It would be good if (a-b) values could be determined for these experiments too, which can be done without modelling the steps.

Reply to DC55

According to this comment, we determined the $a-b$ value by simply comparing the averaged friction coefficients for two velocities for dry experiments under normal stress conditions of 40 and 60 MPa. We added sentences that explain how we determined $a-b$ value for stick-slip behavior in the Method section (lines 262–267 in the marked-up manuscript). Texts in the Result and the caption for Fig. 4 were also modified (lines 343–344 and 361–362 in the marked-up manuscript). Results were also added into Fig. 4 as shown in the next comment.

DC56 in line 242 (Caption for Figure 4)

Please add the "upsteps" vs. "downsteps" in each panel for clarification.

Reply to DC56

According to this comment and Comment 17 by referee #2, we added “upsteps” and “downsteps” in the figure as follows:

(Before)

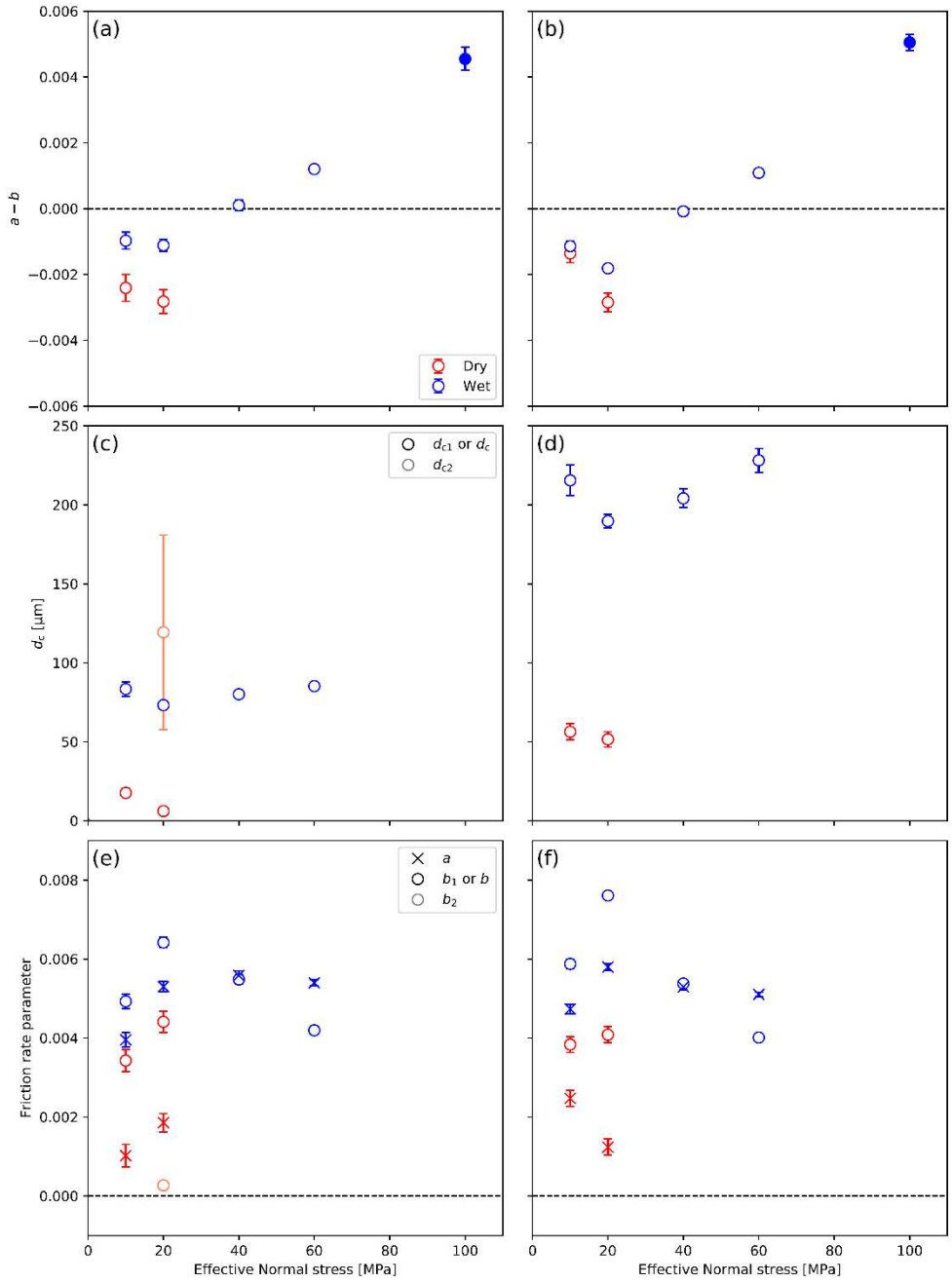
(a)
(b)
(c)
(d)
(e)
(f)
a − b
Dry
Wet
d_{c1} or d_c
d_{c2}
d_c [μm]
a
b_1 or b
b_2
Friction rate parameter
Effective Normal stress [MPa]
Effective Normal stress [MPa]

(After)

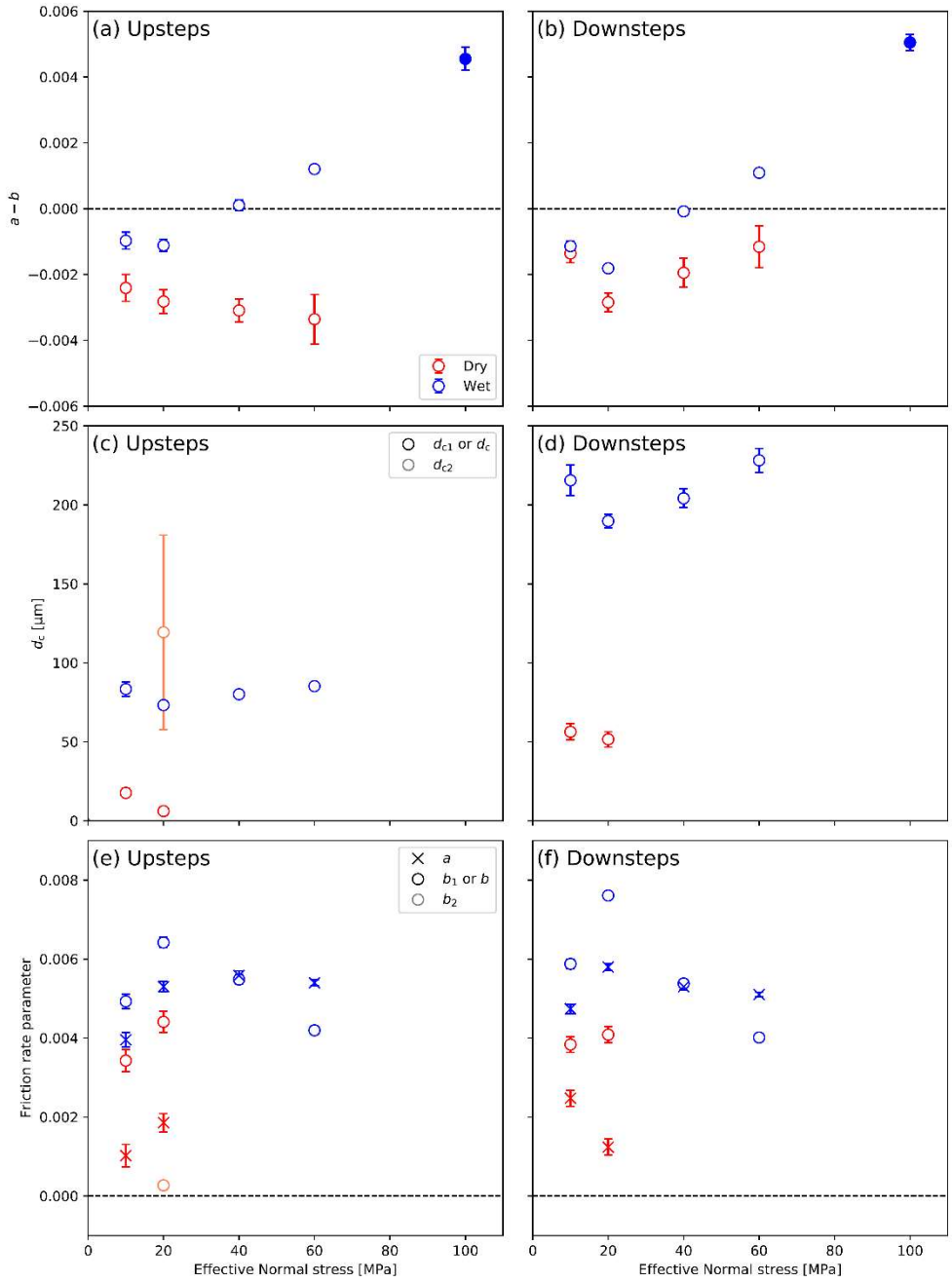

DC57 in line 258

Replace "gouge width shortened" into "gouge thickness decreased."

Reply to DC57

Per this comment, we replaced this phrase with "gouge thickness decreased" and modified all "gouge/shear band width" into "gouge/shear band thickness."

DC58 in lines 267-268

The microstructures do not provide enough evidence to conclude this. In fact, these very low resolution micrographs provide very little information on the deformation processes as individual grains cannot be observed.

Reply to DC58

Both dry and wet cases showed the propagation of Riedel shear, followed by the boundary shear. Plus, as the deformation localized along the boundary shear according to the crystal orientation, we expect that the difference in the entire gouge thicknesses will not affect the overall frictional characteristics. However, as the referee commented, microstructural analyses with higher resolution is needed for clarification. Unfortunately, individual grains could not be observed by polarized or scanning electron microscopes because the grains were very small (70 nm in diameter). Therefore, we modified this sentence to explain the limitation of this study (lines 388–393 in the marked-up manuscript) as follows:

(Before) The narrow width of the gouge in the wet case may be the result of the leaking the sample during the experiment, although the deformation processes of the dry and wet cases do not differ, as shown above.

(After) The narrow thickness of the gouge in the wet case may result from the leakage of the sample during the experiment, but we did not have any mechanism to prevent the gouge from leaking out. The difference in the entire gouge thickness may not affect the overall frictional characteristics because both dry and wet cases showed the Riedel shear development at first, followed by the boundary shear development. Observation of grain contact is needed for clarification, but it was not possible in this study because the grains were very small (70 nm in diameter).

DC59 in line 285

Please clarify.

Reply to DC59

Per this comment, we modified the text (lines 410–411 in the marked-up manuscript) as follows:

(Before) Because the elongation of brucite is length fast (Berman, 1932) and its birefringence is 0.014–0.020 (Deer et al., 2013),

(After) Because brucite has a negative elongation (Berman, 1932) and its birefringence is 0.014–0.020 (Deer et al., 2013),

DC60 in line 295

I do not think that this is true - 10 micron for the dry case vs. 20 micron for the wet case.

Reply to DC60

Per this comment, we modified that description as follows (lines 422–423 in the marked-up manuscript):

(Before) The width of the shear band is 20 μm (Fig. 7d), that is, the same as in the dry case.

(After) The thickness of the shear band is 20 μm (Fig. 7d), which is a little wider than the dry experiments.

DC61 in line 312

Replace "indicating" into "suggesting."

Reply to DC61

Per this comment, we replaced it with "suggesting" (line 443 in the marked-up manuscript).

DC62 in lines 313-314

I believe that this observation was not reported in the Results section?

Reply to DC62

We reported this observation as "The gouge width remained almost constant following the post-yield and in the steady state." in line 384 in the marked-up manuscript, Result section 3.2.1. However, to make it clearer, we rewrite this sentence a follows:

(Before) The gouge width remained almost constant following the post-yield and in the steady state.

(After) The gouge thickness remained almost constant after the post-yield and in the steady state, suggesting that the deformation may localize parallel to the shear deformation, i.e., parallel to the boundary shear.

DC63 in line 315

Replace "confirming that the shear deformation within the gouge occurs" into "consistent with shear deformation localized."

Reply to DC63

Per this comment, we replaced it with "consistent with shear deformation localized" (line 446 in the marked-up manuscript).

DC64 in lines 316-317

This does not make sense - please correct.

Reply to DC64

Per this comment, we rewrote this sentence (lines 448–449 in the marked-up manuscript) as follows:

(Before) friction with a smooth slip surface reduces the friction coefficients

(After) a smooth slip surface reduces the friction coefficient compared to a roughened slip surface

DC65 in line 317

Insert "development of the."

Reply to DC65

Per this comment, we inserted it (line 450 in the marked-up manuscript).

DC66 in line 324

Why is this indirectly?

Reply to DC66

As previous studies suggested that the usage of the nanoparticles could induce the preferred orientation of particles, we would like to express the possibility that the nanoparticle could enhance the observed slip-weakening behavior. However, as we did not test with larger grains, we cannot clarify this. Based on the reason above, we used the word "indirectly" here, but we think using "indirectly" could cause misunderstanding to readers; therefore, we removed this word from the manuscript.

DC67 in line 326 (a comment on discussion)

The microstructures showed Riedel shear as well as boundary shears. How can the Riedel shears be explained if everything would be controlled by the boundary shears as suggested here?

Reply to DC67

As shown in microstructural observations with different shear displacements, the Riedel shear developed at the first stage of the experiment. During the activation of the Riedel shear, the gouge thickness shortened. During the steady state, however, the boundary shear developed, and the

gouge thickness remained constant. This sequence implies that the Riedel shear was no longer active during the steady state. In addition, according to the observation of crystal orientation, we observed the clear alignment of the particle along the boundary shear, but not along the Riedel shear. This observation also supports that the shear deformation localized along the boundary shear. Based on the results described above, we concluded that the boundary shear controls the entire shear deformation in the steady state. We consider that the presence of Riedel shears at the steady state could be remnants of previous deformation structures, which are not active at steady state. Please also refer to the reply to MC3. We expect that arrows along Riedel shears in Figs. 5d and 6e may cause some ambiguities (Comment 19 of referee #2); therefore, we removed those arrows.

DC68 in line 326

Insert "likely."

Reply to DC68

Per this comment, we inserted it (line 459 in the marked-up manuscript).

DC69 in line 337

Replace "weaken" into "decrease."

Reply to DC69

Per this comment, we changed it to "decrease" (line 471 in the marked-up manuscript).

DC70 in line 345 (section title)

Insert "s."

Reply to DC70

Per this comment, we inserted it.

DC71 in line 348

Insert "on brucite."

Reply to DC71

Per this comment, we inserted it (line 483 in the marked-up manuscript).

DC72 in line 349

Insert “and.”

Reply to DC72

Per this comment, we inserted “and” (line 484 in the marked-up manuscript).

DC73 in line 351

Remove “an.”

Reply to DC73

Per this comment, we removed it (line 487 in the marked-up manuscript).

DC74 in line 363

Remove “an.”

Reply to DC74

Per this comment, we removed it (line 500 in the marked-up manuscript).

DC75 in lines 365-366

This is only true if brucite is present in continuous fault strands in which the deformation localizes. I suggest modifying this statement accordingly.

Reply to DC75

According to this comment, we modified the text (lines 502–503 in the marked-up manuscript) as follows:

(Before) Therefore, antigorite and lizardite are not preferably deformed if other weaker minerals, such as brucite, are present.

(After) Therefore, antigorite and lizardite are not preferably deformed if other weaker minerals, such as brucite, are present in continuous fault strands in which the deformation localizes.

DC76 in line 372

Remove “when.”

Reply to DC76

Per this comment, we removed it.

DC77 in line 375

Replace “with” into “at.”

Reply to DC77

Per this comment, we replaced it into “at” (line 514 in the marked-up manuscript).

DC78 in lines 380-384

Please shorten this sentence.

In addition, the last part of this statement is too strong ("brucite is the only mineral that has weak, unstable frictional characteristics"). This is statement is based on laboratory studies, which are not perfect, so weak, unstable frictional characteristics of other minerals cannot be excluded.

Reply to DC78

To shorten this sentence and weaken the statement, we modified it (lines 519–522 in the marked-up manuscript) as follows:

(Before) The distribution of brucite is associated with deformation and the brucite volume is high enough to weaken the bulk strength as discussed in Sect. 4.1; therefore, brucite might be a key mineral controlling the seismic activities in the shallow hydrated mantle wedge because brucite is the only mineral that has weak, unstable frictional characteristics under a wide range of temperature–pressure conditions (Fig. 8).

(After) Although talc is still significantly important for the deformation at the subduction plate interface (Hirauchi et al., 2013), the possible occurrence of brucite and its weak and unstable frictional characteristics implies that brucite might be one of the possibilities to control the seismic activities at the subduction plate interface in the shallow hydrated mantle wedge.

DC79 in line 385

Remove “the.”

Reply to DC79

Per this comment, we removed it (line 527 in the marked-up manuscript).

DC80 in line 423

Insert “range of.”

Reply to DC80

Per this comment, we inserted it (line 571 in the marked-up manuscript).

DC81 in line 424

Insert "s."

Reply to DC81

Per this comment, we inserted it (line 571 in the marked-up manuscript).

Reply to Anonymous Referee #2's comments

Dear referee,

We appreciate your careful review and comments on this manuscript. We took all your comments into consideration as follows. Our replies to your comments are listed below.

Sincerely,
Hanaya Okuda, Ikuo Katayama, Hiroshi Sakuma, Kenji Kawai

Comment 1

This manuscript presents results from friction experiments on Brucite gouge under a range of normal stress and saturation conditions. The results indicate that wet Brucite exhibits a low base friction coefficient and velocity-weakening frictional behavior under low normal stresses. The authors also present microstructural analyses to supplement their experimental results. They use these observations to suggest that Brucite could play an important role in hosting slow earthquakes in a hydrated mantle wedge.

The results are new, interesting and definitely merit publication. However, the authors make multiple strong statements that are not adequately backed up with evidence. Additionally, the manuscript in general and the introduction in particular relies heavily on slow earthquakes in the mantle wedge, without appropriately acknowledging deep slow earthquakes in the plate interface. Finally, the text has multiple grammar and writing errors which need to be corrected prior to publication.

Overall, I believe the manuscript must undergo some moderate/major changes prior to publication. I enumerate my recommendations by line/section below:

1. Abstract line 25-27: "Brucite …. Mantle wedge". This is one example of a strong statement that, in my opinion, is not adequately backed up by the results. This could be one explanation, yes. But to say that this is the 'only mineral' and explains the occurrence of slow earthquakes is bold.

Reply to Comment 1

Thank you for the comment. As your comment and MC1 from referee #1 which both highlighted that the manuscript lacked appropriate acknowledgement on deep slow earthquakes, we added

explanations of slow earthquakes at mantle wedge depth in the first paragraph. Please refer to the replies to MC1 from referee #1 and Comment 6 from referee #2. We modified some parts of our manuscript to tone them down, For example, regarding the sentence "Brucite … mantle wedge.", according to the comment and DC5 from referee #1, we edited the sentence (lines 26–28 in the marked-up manuscript) to tone it down as follows:

(Before) Brucite is found to be the only mineral that has a low friction coefficient and exhibits unstable frictional behavior under hydrated mantle wedge conditions, explaining the occurrence of slow earthquakes in the mantle wedge.

(After) Among serpentinite-related minerals, weak and unstable frictional behavior of brucite under the hydrated mantle wedge conditions may play a role in slow earthquakes at the subduction plate interface in the mantle wedge.

Comment 2

2. Lines 44-49: This is a long sentence that should be broken down for readability.

Reply to Comment 2

We modified the sentence (lines 89–93 in the marked-up manuscript) as follows:

(Before) Despite a variety of previous experimental investigations of the frictional properties of antigorite and talc (Hirauchi et al., 2013; Moore et al., 1997; Moore and Lockner, 2007, 2008; Okazaki and Katayama, 2015; Reinen et al., 1994; Sánchez-Roa et al., 2017; Takahashi et al., 2007; Tesei et al., 2018), brucite has rarely been considered in previous studies compared with other serpentinite-related minerals, which might be due to the fact that it is difficult to detect brucite under natural conditions because of its fine-grained nature (Hostetler et al., 1966).

(After) Many previous experimental studies investigated the frictional properties of antigorite and talc (Hirauchi et al., 2013; Moore et al., 1997; Moore and Lockner, 2007, 2008; Okazaki and Katayama, 2015; Reinen et al., 1994; Sánchez-Roa et al., 2017; Takahashi et al., 2007; Tesei et al., 2018). However, brucite has rarely been considered in previous studies as it is challenging to detect brucite under natural conditions because of its fine-grained nature (Hostetler et al., 1966).

Comment 3

3. Lines 54-55: "Because Brucite is stable….mantle wedges." I understand that 'stable' here does not refer to frictional stability. However, because it is being used in the context of sliding friction, this makes for a very confusing sentence. I recommend some alternate wording to indicate the presence/detectability of Brucite.

Reply to Comment 3

We would use "brucite stably exists" or "thermodynamically stable" instead of just saying "brucite is stable" to avoid confusion. We also modified Discussion as well as Introduction.

Comment 4

4. Lines 56 – 62: "Only a few…temperature". This is a good introduction describing the friction of Brucite. However, it lacks any information about the stress state of these experiments in literature. Since, this manuscript is about the role of normal stress, it would be useful to mention the stresses used for these expts.

Reply to Comment 4

Per this comment, we added the stresses used in previous studies (line 120 in the marked-up manuscript) as follows:

(Before) Only a few previous experimental studies have been conducted on the frictional properties of brucite.

(After) Only a few previous experimental studies under high normal stress conditions of 100 or 150 MPa have been conducted on the frictional properties of brucite.

Comment 5

5. Lines 62-65: Another sentence that could be broken down to enhance readability.

Reply to Comment 5

According to this comment, we modified the sentence (lines 127–130 in the marked-up manuscript) as follows:

(Before) Because the friction coefficient of the serpentinite gouge can be lowered by approximately ~10–15 % due to the presence of brucite (Moore et al., 2001) in addition to velocity-weakening behavior of brucite under certain conditions, the frictional characteristics of brucite might affect earthquake nucleation processes at mantle wedges.

(After) The friction coefficient of a serpentinite gouge can be lowered by approximately ~10–15 % due to the presence of brucite (Moore et al., 2001). The weakness and velocity-weakening behavior of brucite under certain conditions might affect nucleation processes of slow earthquakes at the subduction plate interface in the mantle wedges

Comment 6

6. Lines 65 – 69: "Although….mantle wedges" These statements are made matter-of-factly but the

links between them are not clear to me and don't follow very easily. I don't understand why brucite is key to understanding slow earthquakes just because there have been observations of slow earthquakes at mantle wedge depths. This might also be a good spot to introduce slow earthquakes as a transitional phenomenon between dynamic seismicity and stable creep.

Reply to Comment 6

Thank you for your comment, with which we agree. This part was moved to the first paragraph and modified according to referee #1's comment (MC1 in referee #1's comments; lines 38–51 in the marked-up manuscript). In the modified part, we first mentioned the classical opinion that the serpentinite in the mantle wedge might contribute to the aseismic behavior below the seismogenic zone's downdip limit. Then, we explained the occurrence of slow earthquakes in the mantle wedge, whose mechanisms are still debated but possibly related to the serpentinite layer. Thus, we focused on the frictional properties of serpentinite. These sentences would be followed by reviewing low effective normal stress conditions at the subduction plate interface, and previous experimental studies on serpentinite and brucite in the following paragraphs. After introducing the frictional behavior of brucite, we stated the importance of brucite for the slow earthquakes in the mantle wedge.

In addition to the modification suggested by referee #1 shown above, we added some sentences about the slow earthquakes according to this comment (referee #2 comment 6) in lines 131–138 in the marked-up manuscript.

Comment 7

7. Lines 70 -85: This paragraph is probably better suited near the introduction to the frictional behavior of Brucite. Right now, the authors talk about Brucite friction, then about the mantle wedge, then back to Brucite friction and normal stress.

Reply to Comment 7

According to the comment, we moved a part of this paragraph into the third paragraph (lines 68–79 in the marked-up manuscript) before the paragraph introduces previous studies on brucite friction.

Comment 8

8. Lines 83-85: Again, this role of Brucite is being boldly overstated at this point as the only conceivable possibility.

Reply to Comment 8

According to this comment and the comment DC18 by referee #1, we removed this sentence. Based on this study, we think that brucite may play a key role in the nucleation of slow earthquakes in the mantle wedge. In the Introduction, however, readers cannot access enough information to reach this conclusion; therefore, we removed the sentence from the Introduction.

Comment 9

9. Line 90: Is WAKO a company?

Reply to Comment 9

Yes, WAKO (FUJIFILM Wako Pure Chemical Corporation) is a Japanese company for chemical materials. We modified the text (lines 168–171 in the marked-up manuscript) as follows:

(Before) WAKO

(After) FUJIFILM Wako Pure Chemical Corporation

Comment 10

10. Line 94: What is the thickness of these gouge layers? Also, was there any mechanism to prevent the gouge 'paste' from squeezing out of the sides in the wet experiments?

Reply to Comment 10

At the steady state, gouge thickness was 400 and 150 μm for dry and wet experiments, respectively. As reduction of gouge thickness before the steady state was about 150 and 200 μm for dry and wet experiments, respectively (Figs. 5 & 6), initial gouge thickness was roughly 550 and 350 μm, respectively. We did not have any mechanism to prevent the gouge from squeezing out for the wet experiments; therefore, the gouge thickness for wet experiments is narrower than that for dry ones. We added a sentence explaining we did not have any mechanism in the Method section at lines 190–192 in the marked-up manuscript. We also stated this in the Result (lines 388–389 in the marked-up manuscript).

Comment 11

11. Line 100: How did you ensure/measure saturation? Presumably mixing the brucite with distilled water alone simply ensures that the gouge is wet, not that it is saturated and all the pore volume is filled with water.

Reply to Comment 11

Because we did not place the system in the vacuum condition, it is not easy to ensure the saturated condition in our study. Therefore, we should use "water-wet condition" instead of "water-

saturated" condition. We modified the text as follows (line 190 in the marked-up manuscript):

(Before) water-saturated conditions

(After) water-wet conditions

Please also refer to the DC22 from referee #1.

Comment 12

12. Lines 125-126: Are these cohesion values from literature? If so, please cite your sources.

Reply to Comment 12

The cohesion values were obtained in this study; therefore, we modified the sentences of lines 208–210 in the marked-up manuscript as follows:

(Before) Note that cohesion was not considered because the cohesion stresses were 0.36 and 0.47 MPa for the dry and wet cases, respectively, which are much smaller than the tested normal stress conditions.

(After) Note that cohesion stresses were 0.36 and 0.47 MPa for dry and wet cases, respectively, calculated by linear regression of shear stress and normal stress of all the experiments. Because the obtained cohesion stresses were too small to affect the friction coefficients, the cohesion stress was not considered in this study.

Please note that this modification includes the DC24 by referee #1's comment.

Comment 13

13. Lines 149-150: Not sure if I agree with this entirely. Yes, within the framework of the aging law in sliding of rough interfaces, the dc reflects asperity diameter in some fashion. However, in the context of gouge experiments with a given porosity, one may also consider the alternative interpretation of dc as the width of a localized shear zone (Marone & Kilgore, 1993) as an appealing definition.

Reply to Comment 13

Thank you for the suggestion. We agree with the comment that d_c may be related to the shear localization as proposed by Marone and Kilgore (1993). Based on our microstructural analysis, thickness of the shear band was 10 and 20 μm for the dry and wet experiments, respectively, indicating that the degree of shear localization for the dry experiment was higher than that for the wet experiment. Although we are not sure whether this difference in shear band thickness can quantitatively explain the difference in dc between dry and wet experiments, d_c values for wet experiments were larger than those for dry experiments, consistent with the relationship between the shear localization and d_c. Therefore, we added some sentences about the relationship between d_c value and shear localization in the Method section (lines 245–252 in the marked-up

manuscript), and also added some sentences about the difference between dry and wet experiments in the Results section (lines 422–426 in the marked-up manuscript).

Comment 14

14. Lines 153-154: I understand the point the authors are trying to convey here, but this statement is very strong. Yes, there is an ongoing debate as to the choice of a 'right' constitutive law. However, stating that the value of a – b is 'more' critical needs additional evidence or citations. One might argue that the roles of dc, stiffness k etc. are just as important.

Reply to Comment 14

We agree with this comment. Further, referee #1 left a comment about this sentence (DC31). We would like to use $a-b$ because $a-b$ value is the essential component to control earthquake nucleation processes, but our sentence does not appropriately describe our aim. Therefore, we modified the text (lines 247–252 in the marked-up manuscript) as follows:

(Before) Although there are still debates on the choice of constitutive laws (Bhattacharya et al., 2015, 2017; Marone, 1998), the value of $a-b$ is more critical for seismic activities.

(After) Although there are still debates on the choice of constitutive laws (Bhattacharya et al., 2015, 2017; Marone, 1998), as all constitutive laws give the same result on $a-b$, we calculated the value of $a-b$ by using separately obtained a and b with the aging law. The focus of this study will be the $a-b$ value because it plays an essential role in the nucleation process of earthquakes. However, other parameters like d_c and stiffness are also important to the nucleation process, and therefore, those parameters should be assessed in future studies.

Comment 15

15. Lines 221-223: "The a-b …. Values." Why does an identical a-b value for up and downsteps necessarily imply that normal stress conditions control this? For a given set of velocities, a-b is independent of the normal stress anyway, so I don't understand this connection.

Reply to Comment 15

We agree with this comment and DC53 by referee #1. We cannot strongly say that the normal stress controls the $a-b$ values; therefore, we deleted the sentence and just stated that the $a-b$ values do not differ between upsteps and downsteps (lines 329–330 in the marked-up manuscript) as follows:

(Before) The $a-b$ values obtained for the upsteps and downsteps insignificantly differ (Figs. 4a and b), which implies that the normal stress condition mainly controls the $a-b$

values.

(After) The $a-b$ values obtained for the upsteps and downsteps insignificantly differ (Figs. 4a and b).

Comment 16

16. Lines 231 – 234: "Although…smaller than b1". Yes, b2 is often smaller than b1 and its effect is small, but is dc2 is also smaller? Often, in a 2 state veriable framework, dc2 >> dc1.

Reply to Comment 16

In this study, we observed that d_{c2} is larger than d_{c1} (Fig. 4) as commented. Because we mainly focus on the $a-b$ value in this study, we did not mention the large d_{c2} value in the original manuscript. However, we would like to note the value of d_{c2} as follows (lines 345–348 in the marked-up manuscript):

(Before) Although the second variables b_2 and d_{c2} were introduced in certain experiments (HTB575 and HTB598), their effects on the frictional characteristics are small because the b_2 values are much smaller than b_1 (Fig. 4e and Table S1).

(After) Note that the second variables b_2 and d_{c2} were introduced in two experiments (HTB575 and HTB598). However, their effects on the earthquake nucleation process, that is, $a-b$ value, are small because the b_2 values are much smaller than b_1, although d_{c2} value is much larger than d_{c1} (Fig. 4e and Table S1).

Comment 17

17. Figure 4: Please annotate that column 1 is all upsteps and column 2 is downsteps.

Reply to Comment 17

According to this comment and DC56 by referee #1, we added "upsteps" and "downsteps" in figure 4 as follows:

(Before)

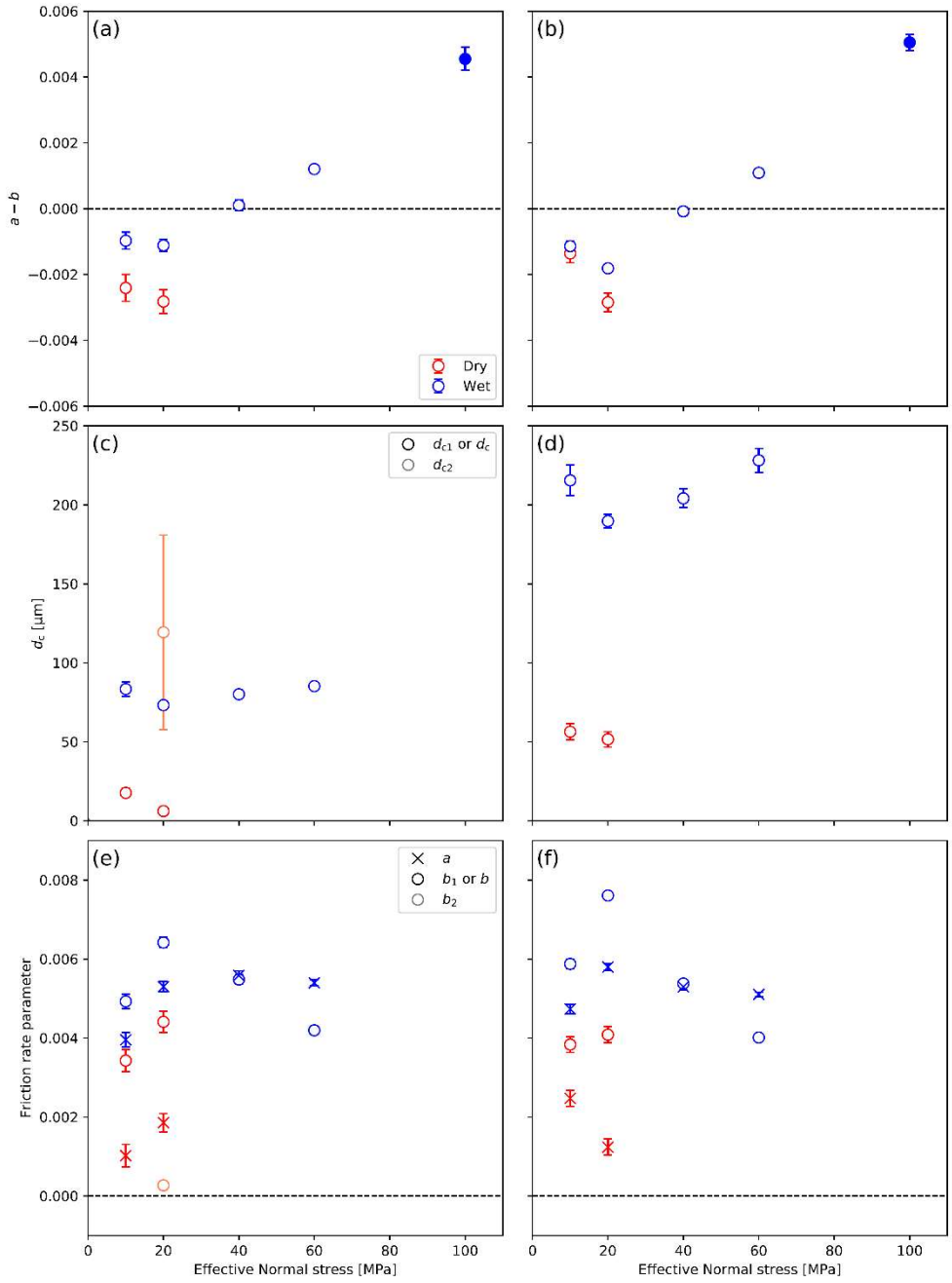
(a)
(b)
(c)
(d)
(e)
(f)
a − b
Dry
Wet
d_{c1} or d_c
d_{c2}
d_c [μm]
a
b_1 or b
b_2
Friction rate parameter
Effective Normal stress [MPa]
Effective Normal stress [MPa]

(After)

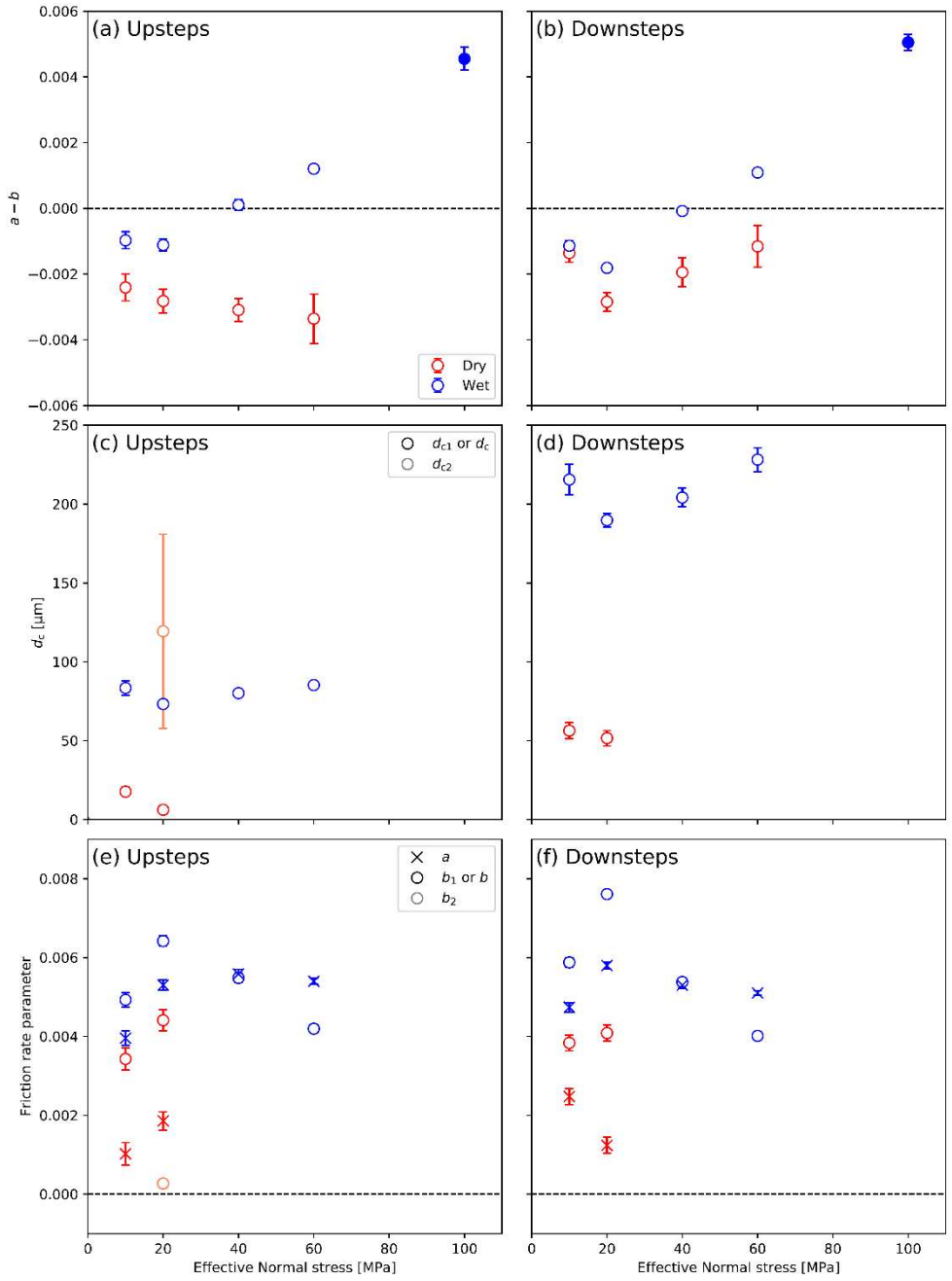

Comment 18

18. Lines 257-268: Many of these observations are also consistent with recent works by Kenigsberg et al. (2019, 2020 – JGR) on clay-rich gouges although they document clear Y and P foliations. This may be worth noting.

Reply to Comment 18

Thank you for letting us know about those works. We added Kenigsberg et al. (2019; 2020) in lines 382–383 in the marked-up manuscript.

Comment 19

19. Lines 310-315: Based on your own sketches in Figs. 5-6, it appears that the deformation could well be accommodated, at least in part, by the Riedel shears. Since there appears to be no additional measurements of gouge compaction/dilation, it seems like the interpretive statements on the location and direction of deformation may be overstated. Also, by stating "constant gouge thickness", do you imply that there was no layer thinning observed in your experiments due to mass loss? This is very surprising.

Reply to Comment 19

Based on Figures 5 and 6, we drew arrows along the Riedel shears at the steady state, leading to some ambiguities that the Riedel shears were still active during steady state. However, according to the observations of crystal orientation at the steady state, we found the alignment of the platy particles only along the boundary shear, showing evidence of the contribution of boundary shear to the deformation at the steady state. Notably, we found no crystal orientation along the Riedel shears, supporting that the deformation is likely to localize along the boundary shear. Hence, we removed arrows along the Riedel shears from Figures 5d and 6c, which may have caused readers to infer that the Riedel shears were still active during the steady state. Please also refer to MC3 and DC67 from referee #1.

Regarding the constant gouge thickness, it is hard to quantitatively say that no mass loss had occurred. After some experiments, however, we "opened" the blocks and confirmed that the whole area of the block surface was filled with brucite gouge. Though a qualitative observation, we think this implies that the mass loss during experiments was little and, therefore, the effect on the experimental results may be negligible.

Comment 20

20. Lines 316-319: Not sure I understand this statement. Anthony and Marone (2005) refer to the smoothness of grain boundary contacts whereas I assume here you refer to boundary shears, which are more or less ubiquitous regardless of the smoothness of grain boundary contacts. I don't believe they are directly comparable as you have done here.

Reply to Comment 20

We referred to Anthony & Marone (2005) here because they compared the forcing blocks with smooth and rough surfaces in addition to the rounded and angular particles. In their study, friction

coefficients became low when forcing blocks with a smooth surface were used, whereas friction coefficients became high when forcing blocks with a rough surface were used. Although it is not so easy to compare the smooth “block surface” and smooth “boundary shear,” we think that smoothness of the boundary shear may play some role in the weakening of the brucite gouge; therefore, we mentioned the work by Anthony & Marone (2005).

Comment 21

21. Section 4.2 : This section is very well thought out and logically organized. I congratulate the authors on this effort. However, it does contain a number of grammar errors which should be thoroughly cleaned up.

Reply to Comment 21

Thank you for your encouraging comment. We appreciate your careful review despite our poor English. The referee #1 also suggested us to improve grammar. After we corrected all suggestions by referee #1, we used an English correction service to improve the manuscript further.

Effect of normal stress on the ~~friction~~ frictional behavior of brucite: Application to slow earthquakes at the subduction plate interface in the mantle wedge

Hanaya Okuda[1,2], Ikuo Katayama[3], Hiroshi Sakuma[4], Kenji Kawai[1]

[1]Department of Earth and Planetary Science, School of Science, University of Tokyo, Bunkyo, 113-0033 Tokyo, Japan

[2]Department of Ocean Floor Geoscience, Atmosphere and Ocean Research Institute, University of Tokyo, Kashiwa, 277-8564 Chiba, Japan

[3]Department of Earth and Planetary Systems Science, Hiroshima University, Higashi-Hiroshima, 739-8526 Hiroshima, Japan

[4]Research Center for Functional Materials, National Institute for Materials Science, Tsukuba, 305-0044 Ibaraki, Japan

Correspondence to: Hanaya Okuda (okuda@aori.u-tokyo.ac.jp)

Abstract

We report the results of friction experiments on brucite under both dry and ~~water-saturated (wet)~~ wet conditions under various normal stresses (10–60 MPa). The ~~steady-state~~ final friction coefficients of brucite were determined to be 0.40 and 0.26 for the dry and wet cases, respectively, independent of the normal stress. Under dry conditions, velocity-weakening behavior was observed in all experiments at various normal stresses. Under wet conditions, velocity weakening was observed at low normal stress (10 and 20 MPa), whereas velocity strengthening was determined at a higher applied normal stress. ~~The microstructural observations~~ Microstructural observations on recovered experimental samples indicate localized deformation within ~~the~~ a narrow shear band, implying that a small volume of brucite can control the bulk frictional strength in an ultramafic setting ~~and significantly change the frictional properties~~. Among serpentinite-related minerals, weak and unstable frictional behavior of brucite under the hydrated mantle wedge conditions may play a role in slow earthquakes at the subduction plate interface in the mantle wedge. ~~Brucite is found to be the only mineral that has a low friction coefficient and exhibits unstable frictional behavior under hydrated mantle wedge conditions, explaining the occurrence of slow earthquakes in the mantle wedge.~~

1. Introduction

Serpentinite is generated by the hydration of ultramafic rocks and has various mineral compositions depending on temperature–pressure conditions of the $MgO–SiO_2–H_2O$ system (Evans et al., 2013). As serpentinite has been observed in various important tectonic settings and is considered to contribute to the weakness of serpentinite-dominant areas, the frictional properties of serpentinite have been investigated for several decades (see Guillot et al., 2015; Hirth and Guillot, 2013 for a review). A large volume of serpentinite is located in the mantle wedge in which olivine-rich rock of the upper mantle is hydrated ~~due~~ by slab-derived water and composes the subduction plate interface as suggested by geological and seismological studies (Bostock et al., 2002; Christensen, 2004; Guillot and Hattori, 2013; Hyndman and Peacock, 2003; Kawahara et al., 2016; Kawakatsu and Watada, 2007; Mizukami et al., 2014; Peacock and Hyndman, 1999; Reynard, 2013). Because of the ~~its~~ mechanical weakness of serpentinite, the relationship between the presence of serpentinite and ~~could contribute to~~ the aseismic behavior below the downdip limit of seismogenic zones has been argued (Hyndman and Peacock, 2003; Oleskevich et al., 1999). However, many recent observations indicated that slow earthquakes, such as Episodic Tremor and Slip (ETS), Slow Slip Events (SSE), or Low-Frequency Earthquakes (LFE), occur at a depth of the mantle wedge in various subduction zones (Audet and Kim, 2016; Obara, 2002; Obara and Kato, 2016; Rogers and Dragert, 2003; Shelly et al., 2006). As those slow earthquakes can trigger or be triggered by huge megathrust earthquakes (Obara and Kato, 2016), the nucleation processes of slow earthquakes are important for understanding seismic activities at subduction zones.

Recent seismological and geological studies expect that several hundreds of meters to kilometers wide layer is serpentinized and foliated along the subduction plate interface, and the deformation of this serpentinite layer is likely to relate to slow earthquakes at a depth of the mantle wedge (Bostock et al., 2002; Calvert et al., 2020; DeShon and Schwartz, 2004; Dorbath et al., 2008; Kawakatsu and Watada, 2007; Nakajima et al., 2009; Ramachandran and Hyndman, 2012; Tarling et al., 2019). Within this foliated

serpentinite layer, both meta-ultramafic and meta-sedimentary blocks are present and metasomatic reactions occur at the boundary between these blocks and the serpentinite matrix (Guillot et al., 2015; Tarling et al., 2019). Such a block-in-matrix structure exhibits complex rheological behavior such that shear stress is controlled by both ductile and brittle deformations of block and matrix depending on the strain rate (Fagereng and den Hartog, 2017; den Hartog and Spiers, 2014; Niemeijer and Spiers, 2007; Tarling et al., 2019). Thus, understanding the deformation properties of both block and matrix is essential to constrain how the subduction plate interface behaves and generates slow earthquakes. This was also underlined by a geological study on the Livingstone Fault. New Zealand (Tarling et al., 2019), which found that the cataclastic slip surface was coated by scaly serpentinite, suggesting that the deformation process of serpentinite is important for brittle deformation as well as widespread ductile deformation at the subduction plate interface.

In addition, near lithostatic pore pressure conditions, which lead~~s~~ to low effective normal stress conditions, have been inferred based on seismic velocity structures at the plate interfaces of several subduction zones where slow earthquakes coincidently occur in the regions such as Cascadia, SW Japan, Central Mexico, and Hikurangi (Audet et al., 2009; Audet and Kim, 2016; Eberhart-Phillips and Reyners, 2012; Matsubara et al., 2009; Shelly et al., 2006; Song and Kim, 2012). This low effective normal stress condition may be correlated to slow earthquakes because frictional deformation becomes dominant, rather than viscous deformation, in terms of shear strength (French and Condit, 2019; Gao and Wang, 2017). Furthermore, the low effective normal stress condition ~~is~~ seems favorable for the nucleation of slow earthquakes (Liu and Rice, 2007, 2009; Rubin, 2008; Segall et al., 2010) and is also consistent with smaller stress drops than regular earthquakes (Ide et al., 2007; Rubinstein et al., 2007, 2008; Schmidt and Gao, 2010). Thus, frictional properties of serpentinite under the low effective normal stress condition likely play an important role in slow earthquakes at the subduction plate interface near the mantle wedge.

Serpentinite in the mantle wedge ~~The mantle wedge~~ is mainly composed of an antigorite–olivine assemblage in ~~the case of~~ warm subduction zones like Cascadia, whereas a brucite–antigorite assemblage dominates in the case of cold subduction zones such as that in NE Japan (Peacock and Hyndman, 1999). Because fluids from subducting slabs have a high SiO_2 content, talc is stable in the vicinity of the slab–mantle boundaries (Hirauchi et al., 2013; Peacock and Hyndman, 1999). ~~The mineral composition of serpentinite has a strong effect on the mechanical behavior of bulk serpentinite because each serpentinite-related mineral, such as antigorite, brucite, and talc, has a different frictional behavior.~~ Serpentinite is made up of serpentinite-related minerals, such as antigorite, brucite, and talc, and as those minerals show different frictional behavior, the frictional properties of each mineral should be understood to interpret the mechanical behavior of bulk serpentinite. Many previous experimental studies investigated the frictional properties of antigorite and talc (Hirauchi et al., 2013; Moore et al., 1997; Moore and Lockner, 2007, 2008; Okazaki and Katayama, 2015; Reinen et al., 1994; Sánchez-Roa et al., 2017; Takahashi et al., 2007; Tesei et al., 2018). However, brucite has rarely been considered in previous studies, as it is challenging to detect brucite under natural conditions because of its fine-grained nature (Hostetler et al., 1966). ~~Despite a variety of previous experimental investigations of the frictional properties of antigorite and talc (Hirauchi et al., 2013; Moore et al., 1997; Moore and Lockner, 2007, 2008; Okazaki and Katayama, 2015; Reinen et al., 1994; Sánchez-Roa et al., 2017; Takahashi et al., 2007; Tesei et al., 2018), brucite has rarely been considered in previous studies compared with other serpentinite-related minerals, which might be due to the fact that it is difficult to detect brucite under natural conditions because of its fine-grained nature (Hostetler et al., 1996).~~ Brucite is not thermodynamically stable when the slab-derived water contains high SiO_2 content, and the mantle wedge may undergo the silica metamorphism (Manning, 1997; Peacock and Hyndman, 1999). However, ~~Recent~~ geological works on the ~~paleo-~~exhumed mantle wedge regions suggested that the silica metamorphism has not occurred widely within the shallow mantle wedge because talc zones or metasomatic reactions are often limited in the narrow part near the meta-sedimentary rocks

(Angiboust and Agard, 2010; D'Antonio and Kristensen, 2004; French and Condit, 2019; Guillot et al., 2009; Kawahara et al., 2016; Mizukami et al., 2014; Nagaya et al., 2020; Reynard, 2013; Tarling et al., 2019). These observations indicate that the serpentinite layer at the subduction plate interface may contain brucite because of low silica metamorphism as brucite itself has sometimes been found (Kawahara et al., 2016; Mizukami et al., 2014) ~~in SW Japan revealed the presence of brucite and suggested that silica metamorphism has not widely occurred within the shallow mantle wedge~~. Hydrothermal experiments also support the finding that the SiO_2 is effectively consumed and brucite can stably exist with antigorite (Oyanagi et al., 2015, 2020). Although deformation may localize at the metasomatic region (Hirauchi et al., 2013; Tarling et al., 2019), the foliated structure of serpentinite matrix implies that the serpentinite layer still accompanies some portion of deformation at the subduction plate interface. ~~In addition, brucite was also detected in ultramafic clasts that erupted from mud volcanoes of the Mariana forearc mantle where the cold Mariana Plate subducts beneath the Philippine Sea Plate (D'Antonio and Kristensen, 2004).~~ Furthermore, as brucite is a sheet-structure mineral, which often shows a low friction coefficient due to weak interlayer bonding, its frictional behavior may play a role in earthquakes at the serpentinite layer (Moore et al., 2001; Moore and Lockner, 2004). ~~Because brucite is stable in the mantle wedge, its frictional properties should be investigated to understand the seismic activities in hydrated mantle wedges.~~

Only a few previous experimental studies under high normal stress conditions of 100 or 150 MPa have been conducted on the frictional properties of brucite. It was shown that brucite has friction coefficients of 0.40–0.46 (dry) or 0.28 (wet), which are lower than those of antigorite (Moore and Lockner, 2004, 2007; Morrow et al., 2000). Regarding the velocity dependence, significant stick-slip behavior has been observed ~~stick-slip behavior is significant~~ for dry brucite at both room and high temperature, implying velocity-weakening behavior. Conversely, wet brucite shows velocity-strengthening behavior at room temperature, which gradually changes to velocity weakening with increasing temperature (Moore et al., 2001; Moore and Lockner, 2007). The friction coefficient of ~~the~~ a serpentinite gouge can be lowered by

approximately ~10–15 % due to the presence of brucite (Moore et al., 2001). The weakness and velocity-weakening behavior of brucite under certain conditions might affect nucleation processes of slow earthquakes at the subduction plate interface in the mantle wedges because velocity-weakening behavior is likely to relate to slow earthquakes as proposed in previous studies. The dilatancy hardening in the velocity-weakening system (Rubin, 2008; Segall et al., 2010), the slip-weakening (Ikari et al., 2013), the transition from the velocity-weakening to velocity-strengthening system at a cut-off velocity (den Hartog et al., 2012; Matsuzawa et al., 2010; Shibazaki and Iio, 2003), or the slow stick-slip (Leeman et al., 2016, 2018; Okazaki and Katayama, 2015) are proposed as mechanisms that generate slow earthquakes. Most of them require the velocity-weakening system to nucleate earthquakes, especially for seismologically detected events like LFEs; therefore, the velocity-weakening behavior of brucite can be suggestive of slow earthquakes at the subduction plate interface.

~~Because the friction coefficient of the serpentinite gouge can be lowered by about ~10–15 % due to the presence of brucite (Moore et al., 2001) in addition to velocity-weakening behavior of brucite under certain conditions, the frictional characteristics of brucite might affect earthquake nucleation processes at mantle wedges. Although the mantle wedge is generally close to the downdip limit of seismogenic zones (Hyndman and Peacock, 2003; Oleskevich et al., 1999), many recent observations indicated slow earthquakes at the depth of the mantle wedge in various subduction zones (Audet and Kim, 2016; Obara and Kato, 2016). Therefore, the weak, unstable frictional behavior of brucite might be the key to understand the occurrence of slow earthquakes at mantle wedges.~~

However, the frictional behavior of brucite at low effective normal stress has not been studied in spite of its potential relationship to slow earthquakes. ~~The effective normal stress is an important parameter that constrains the frictional behavior because the apparent frictional strength of a material decreases with decreasing effective normal stress. Near lithostatic pore pressure conditions, which leads to low effective normal stress conditions, have been inferred based on seismic velocity structures at the plate interfaces of~~

~~several subduction zones where slow earthquakes coincidentally occur such as Cascadia, SW Japan, Central Mexico, and Hikurangi (Audet et al., 2009; Audet and Kim, 2016; Eberhart-Phillips and Reyners, 2012; Matsubara et al., 2009; Shelly et al., 2006; Song and Kim, 2012). Importantly, low effective normal stress is favorable for the nucleation of slow earthquake (Liu and Rice, 2007, 2009; Rubin, 2008; Segall et al., 2010). Although the frictional behavior of brucite at low effective normal stress could be directly related to the occurrence of slow earthquake in the mantle wedge, previous studies have been conducted at high effective normal stresses of 100 or 150 MPa (Moore et al., 2001; Moore and Lockner, 2007) but not at low effective normal stress.~~ In this study, we experimentally investigated the frictional behavior of brucite at various effective normal stresses ranging from 10 to 60 MPa to understand the effect of brucite on the seismic activities at the subduction plate interface in hydrated mantle wedges. ~~Because brucite shows a weak and unstable frictional behavior under a wide range of pressure–temperature conditions, it is a key material controlling the nucleation of earthquakes in hydrated mantle wedges.~~

2. Methods

2.1. Friction experiment

2.1.1. Sample preparation

Brucite nanoparticles with a grain size of 70 nm chemically synthesized by FUJIFILM Wako Pure Chemical Corporation ~~WAKO~~ were used for the friction experiments to simulate its fine-grained nature (Fig. 1). The synthetic samples had a purity of 99.9 % (data from ~~WAKO~~ FUJIFILM Wako Pure Chemical Corporation).

A biaxial testing machine at Hiroshima University, Japan, was used for all friction experiments in this study (Noda and Shimamoto, 2009). ~~Two gouge layers were formed with~~ There are two gouge layers between three gabbro blocks (Fig. 1). The surfaces in contact with gouges were roughened before the

175 experiments using Carborundum (grit 80) to prevent slip between the blocks and sample. All brucite
176 samples were dried in the vacuum oven overnight under 120 °C before the experiments. This temperature
177 was selected to remove adsorbed water and prevent the dehydroxylation of brucite into periclase (MgO).
178 For the dry experiments, ~~the brucite powder was quickly placed in each of the two gouges~~ the brucite
179 powder was quickly sandwiched between the blocks to form the gouge after removing it from the vacuum
180 oven, and the blocks with samples were then put in the testing machine. For the wet experiments, dried
181 brucite was mixed with distilled water ~~until saturation~~ before placing it in the gouges and then sandwiched
182 between blocks.
183

184 **2.1.2. Experimental procedures**

185 Normal stress was horizontally applied on the side blocks, and shear stress was applied vertically
186 by pushing the center block downward (Fig. 1). Before applying shear stress, the desired normal stress was
187 applied to the blocks for 1 h to prevent an effect of the compaction of the gouge during shear deformation
188 (nominally precompaction). For the wet experiments, the blocks and gouges were placed in the tank filled
189 with distilled water for 1 h under a normal stress of 250 kPa before the precompaction with the desired
190 normal stress such that ~~water-saturated~~ water-wet conditions were achieved. Note that as we did not have
191 any mechanism to prevent the gouge from squeezing out for the wet experiment; therefore, the gouge
192 thickness for wet experiments becomes narrower than that for dry ones. After the precompaction, shear
193 stress was applied with a constant load point velocity of 3 μm s^{-1}. Velocity step tests were repeatedly
194 conducted after the shear displacement reached 10 mm by abruptly increasing the load point velocity to 33
195 μm s^{-1} and decreasing it to 3 μm s^{-1} after ~~sliding of~~ a shear displacement of 1 mm (Fig. 2). The normal stress
196 conditions of 10, 20, 40, and 60 MPa were tested for both the dry and wet cases to study the influence of
197 effective normal stress. In addition, several experiments were conducted with different total shear

displacements to investigate the evolution of the gouge microstructure in both the dry and wet experiments (Table 1).

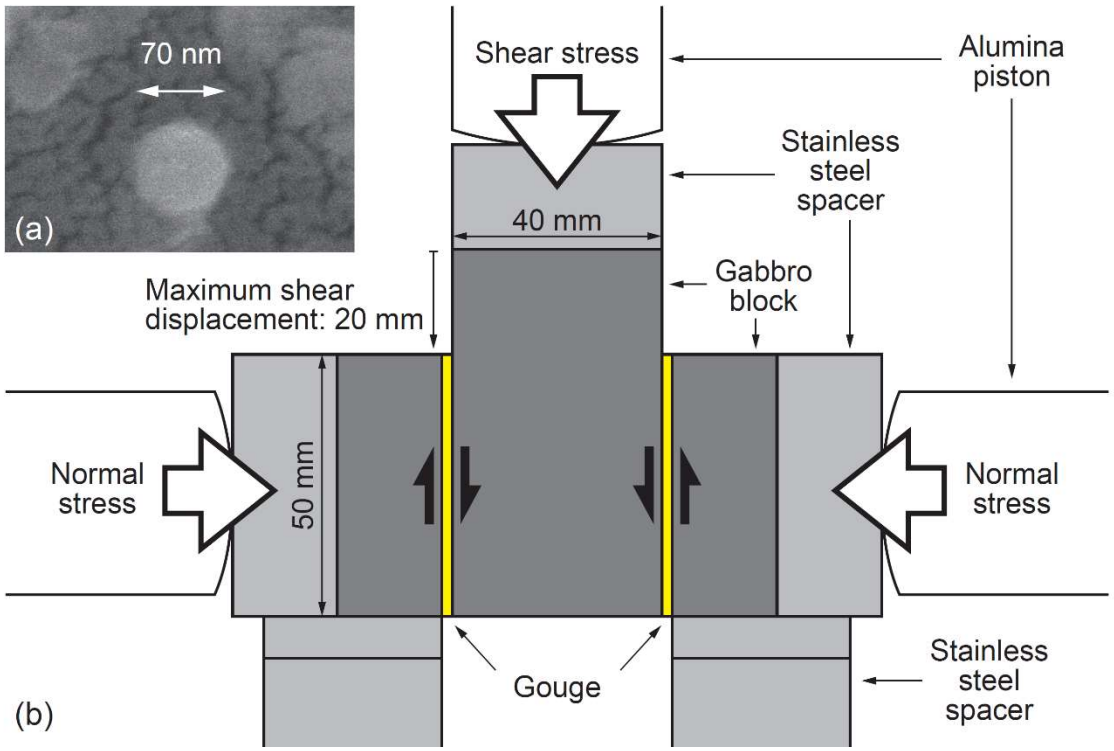

Figure 1: (a) SEM micrograph of synthetic brucite used in this study. ~~The scale bar is 100 nm.~~ (b) Schematic view of the biaxial testing machine used in this study.

2.2. Data analysis

2.2.1. Mechanical data

The friction coefficient μ was calculated from the ratio of the shear stress to the normal stress. Note that cohesion stresses were 0.36 and 0.47 MPa for dry and wet cases, respectively, calculated by linear regression of shear stress and normal stress of all the experiments. Because the obtained cohesion stresses were too small to affect the friction coefficients, the cohesion stress was not considered in this study. ~~Note that cohesion was not considered because the cohesion stresses were 0.36 and 0.47 MPa for the dry and wet~~

cases, respectively, which are much smaller than the tested normal stress conditions. The shear displacement was corrected using the stiffness of the testing machine (4.4×10^8 N m^{-1}). The velocity step tests were analyzed using the rate- and state-dependent friction (RSF) law (Dieterich, 1979; Ruina, 1983). Before conducting the following analyses, the friction coefficient versus the displacement curve was detrended for the slip-weakening trend, which was obtained from the friction data in the second half of each velocity step of 500 μm shear displacement. The slip dependency, which was calculated from the later part of each velocity step test with a shear displacement of 500 μm, was detrended before conducting the following analyses. Detrended data were fitted to the following the RSF law:

$$\mu = \mu_0 + a \ln\left(\frac{V}{V_0}\right) + b_1 \ln\left(\frac{V_0\theta_1}{d_{c1}}\right) + b_2 \ln\left(\frac{V_0\theta_2}{d_{c2}}\right), \quad (1)$$

where a, b_1 and b_2 are nondimensional parameters, μ_0 is the steady-state friction coefficient before the velocity step, V_0 and V are the sliding velocities before and after the velocity step, d_{c1} and d_{c2} are the characteristic slip distances, and θ_1 and θ_2 are the state variables. We estimated the effect of elastic interaction due to the machine stiffness on V using the following relationship: The transition of V was calculated by the following relationship:

$$\frac{d\mu}{dt} = k(V_{lp} - V), \quad (2)$$

where V_{lp} is the load point velocity, which was abruptly changed, and k is the system stiffness, which was treated as an unknown parameter (in μm^{-1}). The Dieterich (aging) law (Dieterich, 1979; Marone, 1998; Ruina, 1983) was used for the state variable in this study.

$$\frac{d\theta_i}{dt} = 1 - \frac{V\theta_i}{d_{ci}}, i = 1, 2 \quad (3)$$

A MATLAB code, RSFit3000, developed to fit the velocity step and slide hold slide tests (Skarbek and Savage, 2019) was used for the analyses of velocity step tests. Second variables b_2, θ_2, and d_{c2} (Blanpied et al., 1998) were only introduced when the experimental data were poorly fitted (upsteps of HTB575 and HTB598; Fig. 4); otherwise, b_2 and θ_2 were treated as 0. The value of $a - b$ ($a - b_1 - b_2$, or $a - b_1$)

was then calculated for each step, which describes the instability of the simulated fault: the state of fault is defined as velocity strengthening and stable when $a-b$ is positive, whereas it is defined as velocity weakening and potentially unstable when $a-b$ is negative. Note that d_c values for the velocity steps whose velocities decreased from 33 to 3 μm s^{-1} (downsteps) are larger than those for the velocity steps whose velocities increased from 3 to 33 μm s^{-1} (upsteps). ~~Note that d_c for the downsteps is larger than that for the upsteps.~~ Because we chose to use the Dieterich (aging) law to fit the RSF law, d_c ~~reflects the contact diameter of the asperity contact~~ reflects the diameter of the contact area between grains (Dieterich, 1979; Ruina, 1983). When the load point velocity is 3 μm s^{-1}, the lifetime of one ~~asperity contact~~ contact area ~~becomes~~ is longer than that with a load point velocity of 33 μm s^{-1}. Therefore, the contact diameter, d_c, for the load point velocity of 3 μm sec^{-1} (downsteps) ~~becomes~~ is larger than that for 33 μm s^{-1} (upsteps). In addition, d_c is also considered to reflect the shear localization (Marone and Kilgore, 1993); when the shear localizes, d_c decreases. Hence, the difference in d_c has qualitative information on the shear localization within the gouge. Although there are still debates on the choice of constitutive laws (Bhattacharya et al., 2015, 2017; Marone, 1998), as all constitutive laws give the same result on $a-b$, we calculated the value of $a-b$ by using separately obtained a and b with the aging law. The focus of this study will be the $a-b$ value because it plays an essential role in the nucleation process of earthquakes. However, other parameters like d_c and stiffness are also important to the nucleation process, and therefore, those parameters should be assessed in future studies. ~~Although there are still debates on the choice of constitutive laws (Bhattacharya et al., 2015, 2017; Marone, 1998), the value of $a-b$ is more critical for seismic activities.~~

When the system is velocity weakening, that is, $a-b$ is negative, it starts to vibrate automatically (stick-slip) when the system stiffness is lower than ~~the~~ a critical stiffness, whereas conditionally stable sliding is achieved when the system stiffness is higher than ~~the~~ a critical stiffness. The critical stiffness k_c can be described as follows when quasi-static stick-slip behavior is assumed:

$$k_c = \frac{N(b-a)}{d_c}, \quad (4)$$

where N is the applied normal force (Ruina, 1983). Thus, as the normal force N applied to the velocity-weakening system increases, the system starts to show stick-slip behavior. In other words, the occurrence of stick-slip represents that the system is velocity-weakening. We determined the $a-b$ value for dry experiments with normal stresses of 40 and 60 MPa by simply comparing the averaged friction coefficients during the stick-slip behavior for two velocities based on the following relationship:

$$a - b = \frac{\Delta\mu_{ss}}{\Delta \ln V}, \quad (5)$$

where $\Delta\mu_{ss}$ and $\Delta \ln V$ are variations in the steady-state friction coefficient and the sliding velocity in the log scale, respectively. In this case, neither a, b, nor d_c can be determined.

2.2.2. Microstructure

In the case of sheet-structure minerals, the friction between basal planes of the crystals [(0001) plane for brucite] is thought to be significant due to their weak bonding. The shear surfaces of the samples recovered from friction experiments using sheet-structure minerals often show smooth surfaces ~~based on~~ composed of platy particles aligned parallel to the sliding direction (Moore and Lockner, 2004). Further, according to the experiments with natural samples ~~Under natural~~ conditions, the aligned platy particles of interconnected talc were reported to contribute to the low friction coefficient of ~~the~~ low angle normal faults (Collettini et al., 2009). ~~The experimentally determined friction coefficients of single crystalline muscovite and chlorite are much smaller than those of powdered polycrystalline samples (Horn and Deere, 1962; Kawai et al., 2015; Niemeijer, 2018; Okamoto et al., 2019).~~

Because these experiments indicate that the crystal orientation within the gouge has a significant effect on the friction coefficients of sheet-structure minerals, observations of thin sections of recovered samples were conducted after the experiments (Table 1) to investigate the effects of the deformation

structures and crystal orientation within the gouges on the frictional behaviors. After the experiment, we impregnated the gouge and the blocks with epoxy resin to keep the deformation structures within the gouge. Thin sections parallel to the shear direction and normal to the gouges with a thickness of 30 μm were prepared from the impregnated samples. The scanning electron microscope (SEM, JEOL JXA-8900 at the Atmosphere and Ocean Research Institute, University of Tokyo, Japan) was used for the observation of to observe the microstructures of the gouges. An accelerating voltage of 15 kV and a beam current of 10.0 nA were used for all backscattered electron (BSE) observations. The crystal orientation was determined with a polarizing microscope at the University of Tokyo, Japan.

3. Results

3.1. Mechanical behaviors

3.1.1. Friction coefficients

In general, both dry and wet experiments initially show high friction coefficients at a shear displacement of 1.5–2 mm (hereafter peak friction coefficients) followed by slip-weakening trends lasting about 10 mm shear displacement toward the steady state with a shear displacement of about 10 mm towards the steady state (Figs. 2 and S1). The steady state final friction coefficients at a shear displacement of ~20 mm for dry and wet conditions under all normal stress conditions were 0.40±0.04 and 0.26±0.03, 0.40(4) and 0.26(3), respectively (Table 1). These steady-state final friction coefficients are mostly independent of the applied normal stress (Fig. 3) and consistent with previous experimental results, that is, 0.38-0.46 and 0.28 for dry and wet brucite at an applied normal stress of 100 MPa at room temperature, respectively (Moore and Lockner, 2004, 2007). The friction coefficient for dry experiments is also close to the theoretical value of 0.30±0.03 0.30(3) (Okuda et al., 2019). Note that the peak friction coefficient of wet brucite at an effective normal stress of 60 MPa is high because of sudden stress drops in the initial stage of

the shear displacement (Fig. S1). As this data may include some experimental artifacts, we do not use this peak value for 60 MPa normal stress in this study.

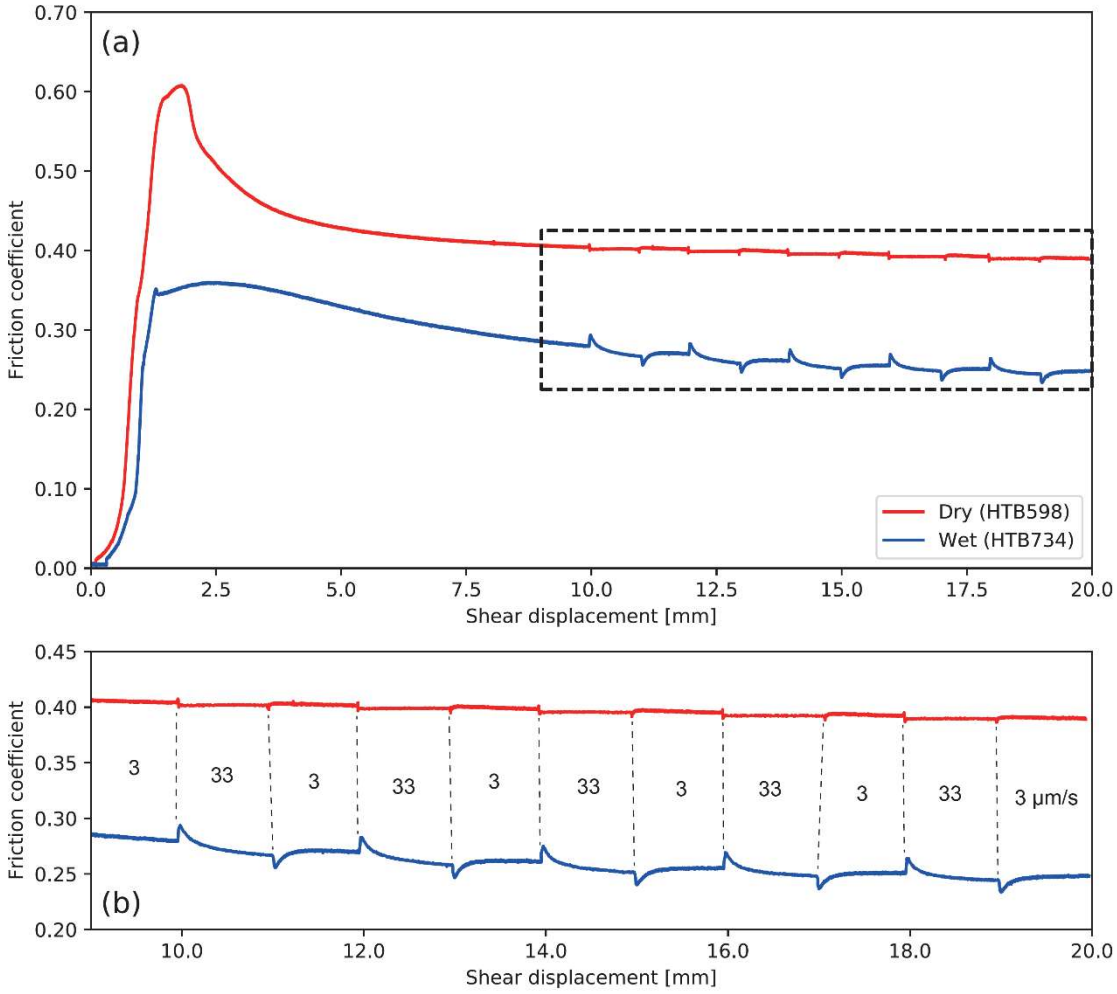

Figure 2: (a) Friction coefficients for dry (HTB598) and wet (HTB734) experiments at a normal stress of 20 MPa. Slip-weakening behavior was observed after the peak under both dry and wet conditions. (b) Enhanced view of velocity step sequences as indicated by the dotted square in (a). The velocities at given shear displacements are displayed between two lines.

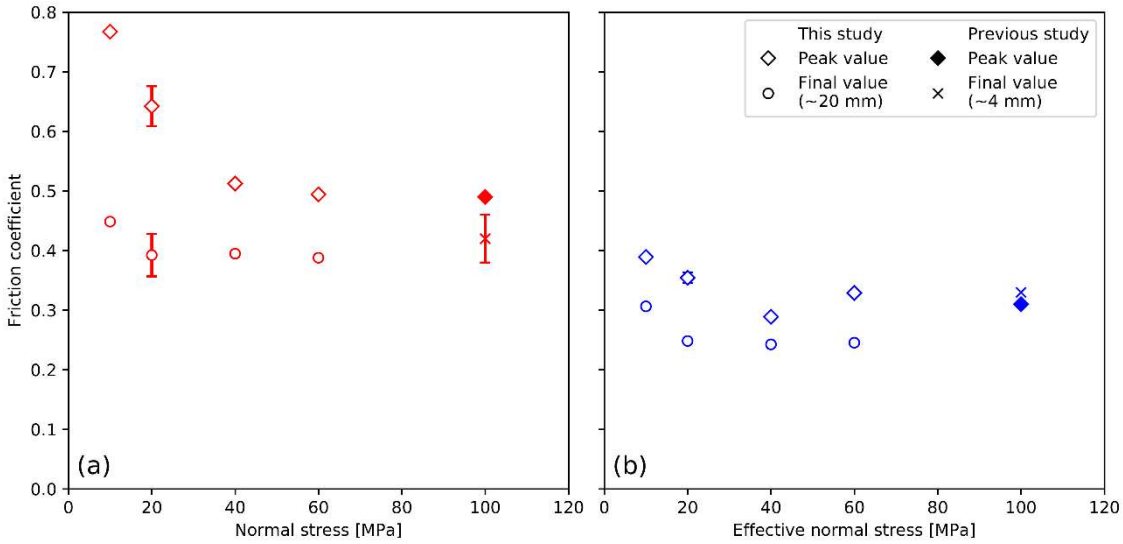

Figure 3: Relationship between normal stress and the peak or ~~steady-state~~ final friction coefficients for the dry (a) and wet (b) experiments. Data at a normal stress of 100 MPa were obtained from previous experiments (Moore et al., 2001; Moore and Lockner, 2004, 2007; Morrow et al., 2000). The ~~steady-state~~ final friction coefficients do not show a clear trend with normal stress ~~insignificantly depend on the applied normal stresses~~. For this study, the error bar represents the one-sigma standard deviation among multiple data. For 100 MPa dry data, the ~~steady state value~~ final friction coefficient and the error bar denote the averaged value of stick-slip behavior and its amplitude, respectively. Note that the peak friction coefficient of wet brucite at an effective normal stress of 60 MPa is high because of sudden stress drops in the initial stage of the shear displacement (Fig. S1). As this data may include some experimental artifacts, we do not use this peak value in this study.

3.1.2. Velocity dependencies

For wet experiments, negative $a-b$ values were observed at low normal stresses of 10 and 20 MPa (Figs. 4a and b). However, the $a-b$ values became almost neutral at 40 MPa and positive at 60 MPa. A positive $a-b$ value was consistent with the previous experiments on wet brucite at an effective normal stress of 100 MPa (Moore et al., 2001; Moore and Lockner, 2007). The $a-b$ values obtained for the upsteps and downsteps insignificantly differ (Figs. 4a and b)~~, which implies that the normal stress condition mainly controls the $a-b$ values~~. ~~The constitutive parameter a insignificantly depends on the applied normal stress, whereas b decreases as the normal stress increases, leading to the transition from negative~~

~~to positive $a - b$ values (Figs. 4e and f).~~ In the experiments with normal stress conditions of 20, 40, and 60 MPa, the constitutive parameter a is almost constant with 0.0054 for both upsteps and downsteps, whereas b decreases from 0.0064 to 0.0042 and from 0.0076 to 0.0040 for upsteps and downsteps, respectively, as the normal stress increases (Figs. 4e and f). Accordingly, we concluded that the decrease in b induces the transition from negative to positive $a - b$. The d_c values at different effective normal stresses insignificantly differ (Figs. 4c and d).

For dry experiments, negative $a - b$ values were obtained at ~~normal stresses of 10 and 20 MPa~~ all normal stress conditions (Figs. 4a and b). When the normal stress was higher than 40 MPa, stick-slip behavior was observed~~, which implies a negative sign of $a - b$~~. This unstable stick-slip behavior was also ~~observed~~ reported in the case of the dry experiment at a higher normal stress of 100 MPa (Moore and Lockner, 2004; Morrow et al., 2000). No information on a, b, and d_c values for 40 and 60 MPa experiments was obtained because of the stick-slip behavior. As shown in the wet conditions, larger d_c values were observed for the downsteps (Figs. 4c and d). Note that the second variables b_2 and d_{c2} were introduced in two experiments (HTB575 and HTB598). However, their effects on the earthquake nucleation process, that is, $a - b$ value, are small because the b_2 values are much smaller than b_1, although d_{c2} value is much larger than d_{c1} (Fig. 4e and Table S1). ~~Although the second variables b_2 and d_{c2} were introduced in certain experiments (HTB575 and HTB598), their effects on the frictional characteristics are small because the b_2 values are much smaller than b_1 (Fig. 4e and Table S1).~~

The constitutive parameters a and b and critical slip distance d_c of the dry and wet experiments significantly differ. The a, b, and d_c values of the wet experiments are larger than those of the dry experiments (Fig. 4). The critical slip distances d_c of the upsteps and downsteps under wet conditions were 5–15 times and 3–4 times larger than those under dry conditions, respectively.

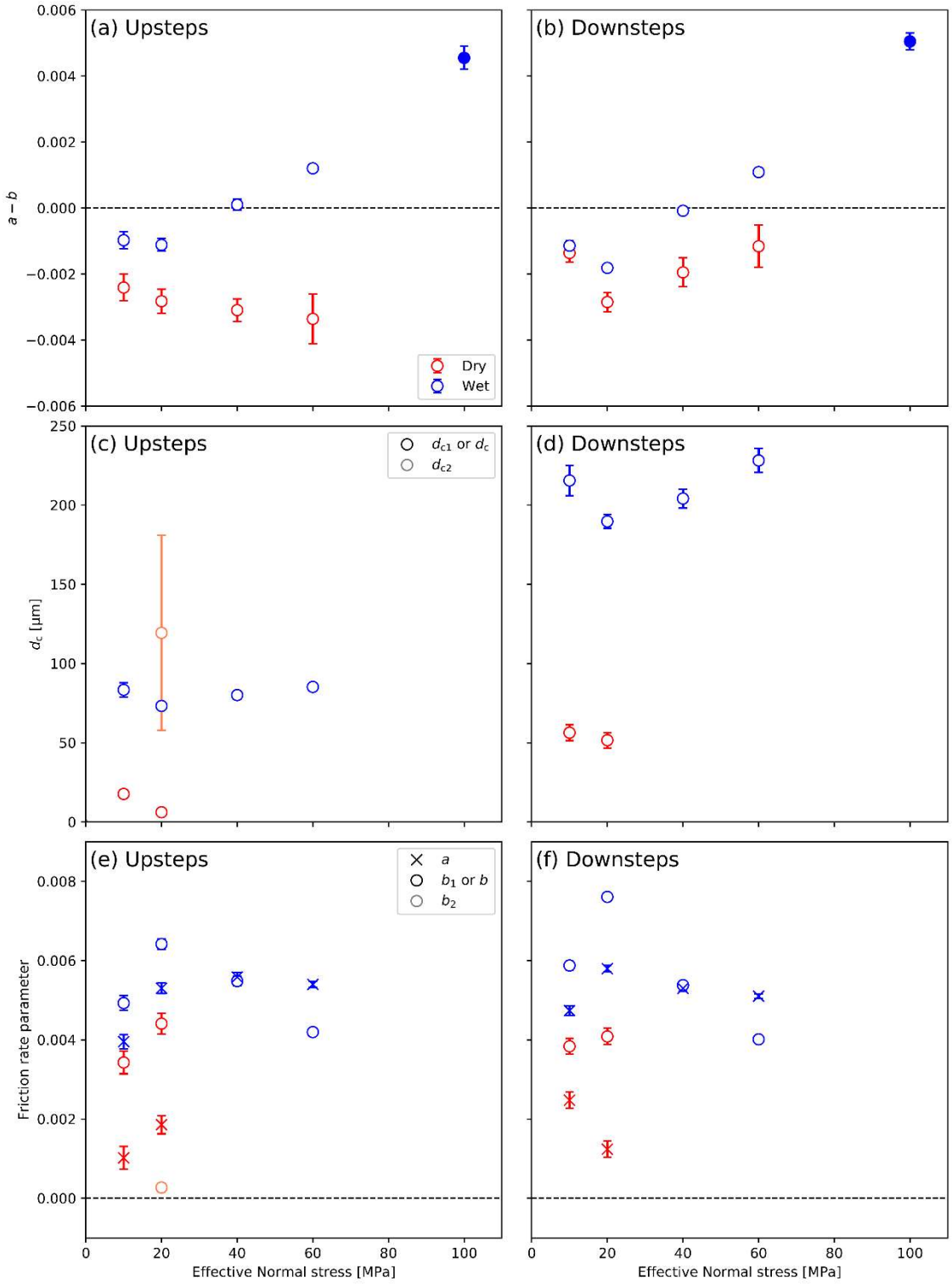

Figure 4: Results of the velocity step tests. Values of $a-b$ for upsteps (a) and downsteps (b), d_c for upsteps (c), and ~~for~~ downsteps (d), a and b for upsteps (e), and ~~for~~ downsteps (f). The errors represent the one-sigma standard deviations of all upsteps or downsteps under each experimental condition, including the errors of the nonlinear least-square fitting processes. The $a-b$ values at a normal stress of 100 MPa were obtained from a

previous study (solid symbol; Moore et al., 2001). Because stick-slip behavior was observed in the dry experiments at normal stresses of 40 and 60 MPa, $a - b$ values were calculated by eq. 5 (Sect. 2.2.1). Second variables b_2 and d_{c2} were introduced for upsteps of the dry experiments at a normal stress of 20 MPa.

3.2. Microstructure

3.2.1. Evolution of deformation structures

As all samples (both dry and wet) showed a peak value followed by a transition into the steady state ~~peak and steady states~~, we chose shear displacements before the peak friction coefficient (pre-yield), after the peak friction coefficient (post-yield), and in the steady state (10 mm) to study the evolution of the deformation structures. Note that the steady state may not be achieved at a shear displacement of 10 mm, but as the final friction coefficients were similar to the friction coefficients at 10 mm shear displacement, here we used the term "steady state" and considered that the microstructure at 10 mm shear displacement might be consistent with the steady state. We followed the description of the microstructure of a sheared gouge by Logan et al. (1979). The results for the dry and wet experiments are shown in Figs. 5 and 6, respectively.

Before the shear loading, no shear structure was observed (Fig. 5a). When the shear force was loaded, the Riedel shear propagated in the pre-yield regime, and the gouge thickness decreased ~~width shortened~~ rapidly at first (Figs. 5b and 6a). Subsequently, the boundary shear started to develop in the post-yield (Figs. 5c and 6b). In the steady state, the boundary shear was created, ~~by the gouge~~ and the Riedel shear tilted subparallel to the boundary shear (Figs. 5d and 6c). The surfaces of the gabbro blocks were filled with brucite, and the boundary shear was much smoother than the original block surface. These observations are consistent with ~~those of~~ previous studies (Haines et al., 2013; Kenigsberg et al., 2019, 2020; Logan et al., 1992; Marone, 1998), although clear Y shear and P foliation were not observed in this study. ~~The gouge width remained almost constant following the post-yield and in the steady state.~~ The gouge thickness remained almost constant after the post-yield and steady state, suggesting that the

deformation may localize parallel to the shear deformation, i.e., parallel to the boundary shear. The ~~width~~ thickness of the entire gouge in the steady state was 400 and 150 μm in the dry and wet cases, respectively (Figs. 5d and 6c). The narrow thickness of the gouge in the wet case may result from the leakage of the sample during the experiment, but we did not have any mechanism to prevent the gouge from leaking out. The difference in the entire gouge thickness may not affect the overall frictional characteristics because both dry and wet cases showed the Riedel shear development at first, followed by the boundary shear development. Observation of grain contact is needed for clarification, but it was not possible in this study because the grains were very small (70 nm in diameter). ~~The narrow width of the gouge in the wet case may be the result of the leaking the sample during the experiment, although the deformation processes of the dry and wet cases do not differ, as shown above.~~

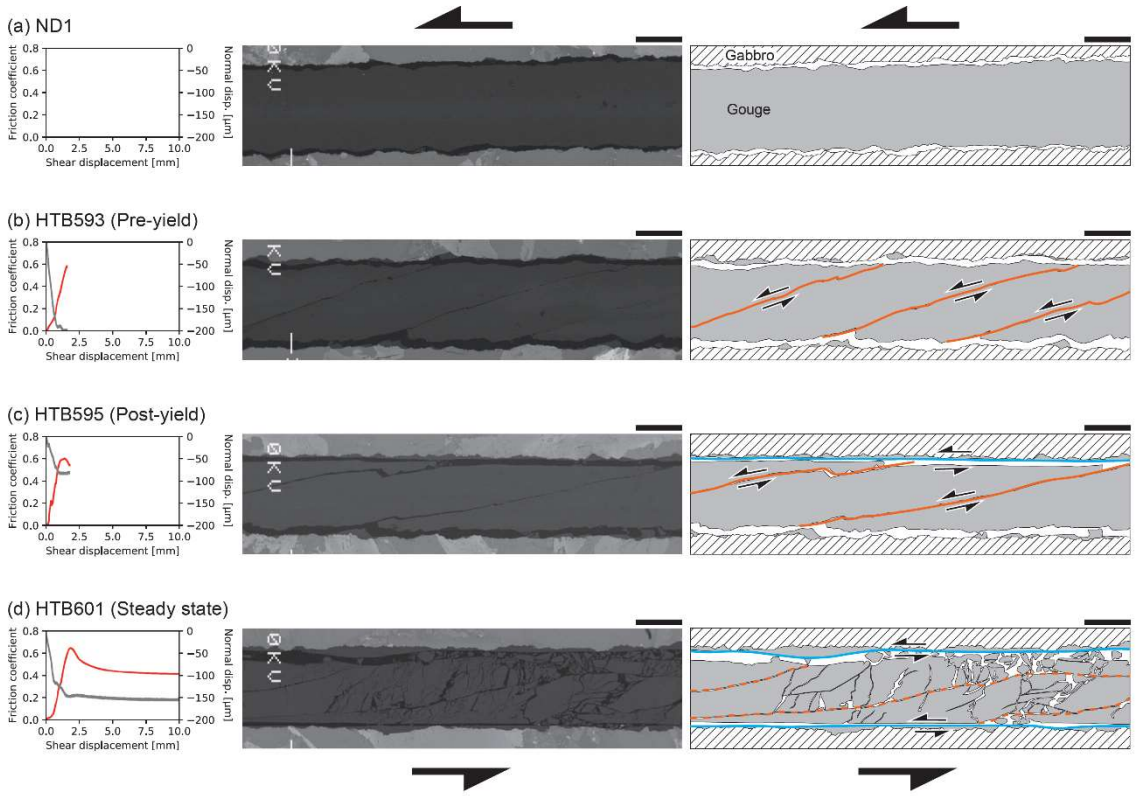

Figure 5: Backscattered electron (BSE) images showing the deformation of gouges (center) and corresponding interpretive sketches (right) of the dry experiments. The friction coefficients and normal displacement are shown in the left panels using colored and gray lines. The orange lines, blue lines, gray area, hatched area, and white

area in the sketches correspond to the Riedel shear, boundary shear, brucite gouge, gabbro block, and epoxy resin, respectively. The orange dot lines are the Riedel shears, which may not be active. The arrows represent the slip directions. The scale bars represent 200 µm.

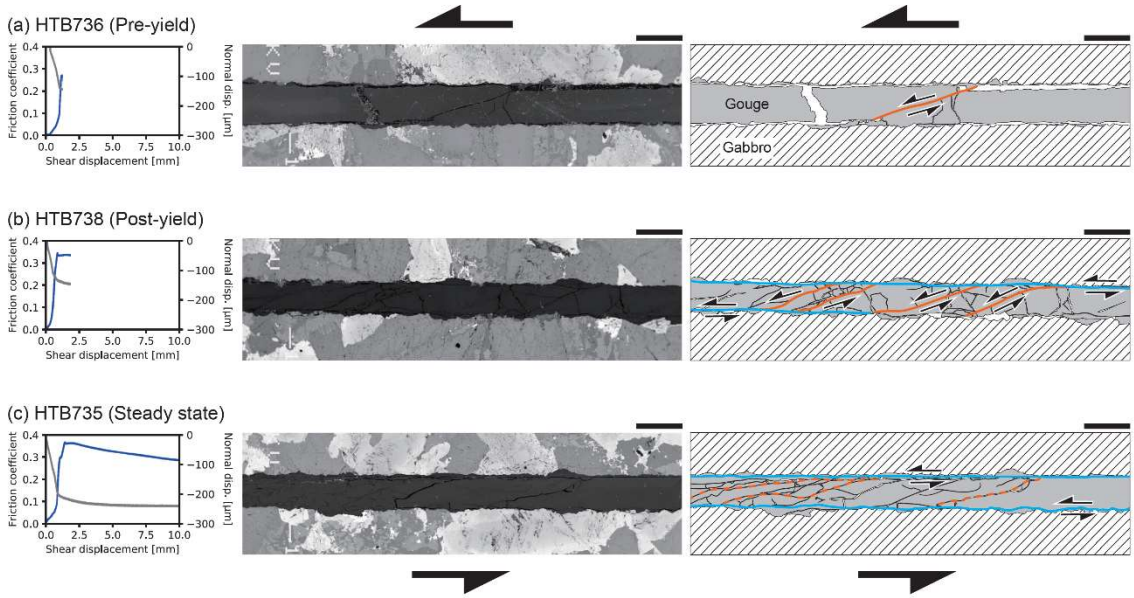

Figure 6: Backscattered electron (BSE) images showing the deformation of gouges (center) and corresponding interpretive sketches (right) of the wet experiments. See Fig. 5~~6~~ for descriptions.

3.2.2. Crystal orientation

Because brucite has a negative elongation (Berman, 1932) and its birefringence is 0.014–0.020 (Deer et al., 2013), ~~Because the elongation of brucite is length fast (Berman, 1932) and its birefringence is 0.014–0.020 (Deer et al., 2013),~~ the interference color of brucite under crossed nicols with the sensitive color plate inserted becomes second-order blue or first-order yellow when the *c* axis of brucite is normal or parallel to the X′-direction of the sensitive color plate, respectively.

In the dry sample (HTB601; Figs. 7a and 7b), a second-order blue line can be observed parallel to the smooth boundary shear~~. This implies~~, implying that the basal (0001) plane of the brucite particles is aligned along the boundary shear parallel to the shear direction. We did not observe any alignment along

the Riedel shears, suggesting that deformation along the Riedel shears cannot be dominant at the steady state. Based on the magnified view, the brucite particles are oriented within 10 μm around the boundary shear (Fig. 7b). Because the purple area indicates that the brucite particles are randomly oriented, the shear strain can be localized within a ~~width~~ thickness of 10 μm. Hereafter, we call this oriented area "shear band." In the wet samples, the crystals are also oriented along the boundary shear (Figs. 7c and 7d). The ~~width~~ thickness of the shear band is 20 μm (Fig. 7d), which is a little wider than that for the dry experiments~~, that is, the same as in the dry case~~. This observation is consistent with the relationship between the shear localization and d_c value (Marone and Kilgore, 1993): the degree of shear localization for the dry sample is higher than that for the wet sample, and d_c for dry sample was smaller than for wet sample (Fig. 4). Note that detailed transmission electron microscopy is required in future studies to confirm the crystal orientation and shear band ~~width~~ thickness, ~~similar to~~ as shown in previous studies (Verberne et al., 2014a; Viti, 2011).

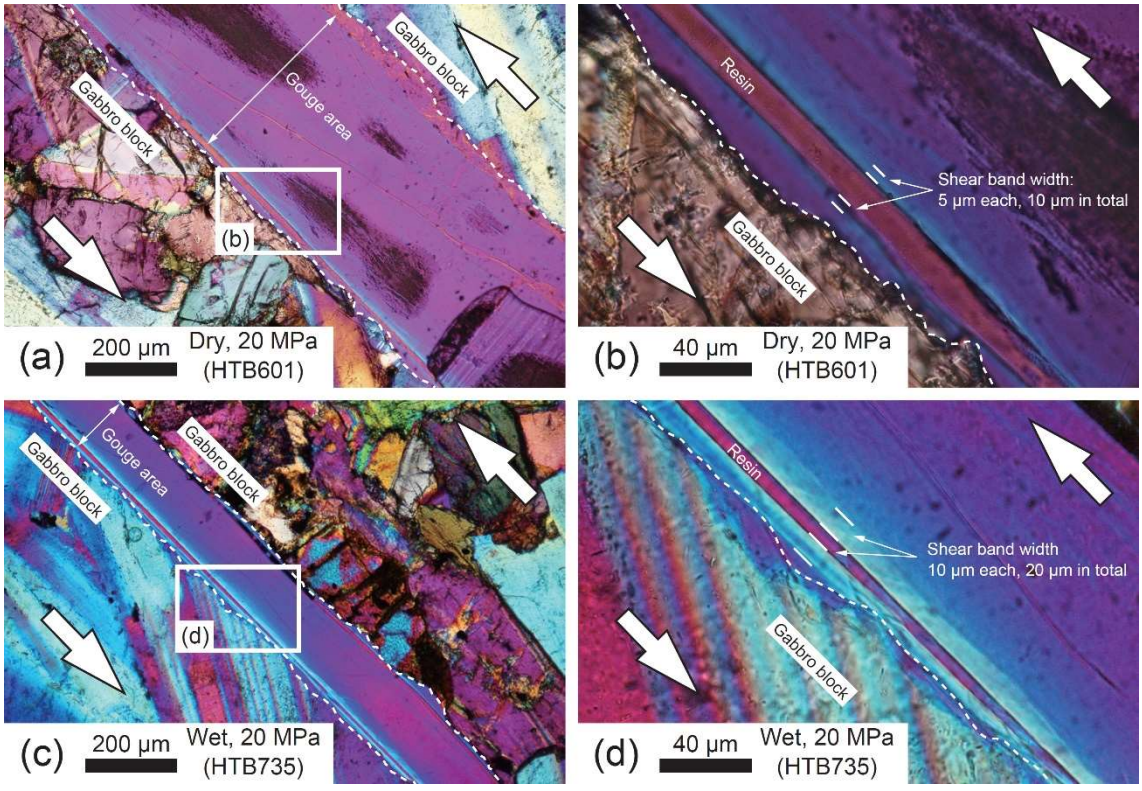

Figure 7: Observation of the crystal orientation using the polarizing microscope under crossed nicols with the sensitive color plate. The arrows indicate the shear direction. The X′-direction of the sensitive color plate is parallel to the shear direction. (a) Dry experiment with 20 MPa normal stress (HTB601). (c) Wet experiment with 20 MPa normal stress (HTB735). (b and d) Magnified views of (a) and (c), respectively. The shear band ~~widths~~ thicknesses are indicated in the figures. The white dashed line represents the boundary between the gabbro block and the brucite gouge.

4. Discussion

4.1. Mechanical weakness of a small amount of brucite

Based on the microstructural observations in Sect. 3.2, the boundary shear is smooth, filling the rough surface of the gabbro block as a "fault mirror" (Siman-Tov et al., 2013). The brucite particles are aligned along the boundary shear, ~~indicating~~ suggesting that the deformation within the narrow shear band is responsible for most of the deformation of the gouge during the steady state. In addition, the constant gouge thickness during the steady state suggests that the gouge deformation occurs parallel to the shear direction, consistent with shear deformation localized ~~confirming that the shear deformation within the gouge occurs~~ within the shear band.

Because previous studies showed that a smooth slip surface reduces the friction coefficient compared to a roughened slip surface ~~friction with a smooth slip surface reduces the friction coefficients~~ (Anthony and Marone, 2005), the development of the smooth boundary shear observed in this study would reduce the friction coefficient with increasing shear displacement (Haines et al., 2013). In addition, the slip between the basal planes of sheet-structure minerals also plays an important role for weak friction because the friction between single crystals of sheet-structure minerals has a lower friction coefficient than that of powdered samples (Horn and Deere, 1962; Kawai et al., 2015; Niemeijer, 2018; Okamoto et al., 2019). Based on the observed alignment of the basal plane of brucite within the shear band, the friction between the basal planes of brucite crystals might enhance the weak friction of brucite. Because the preferred planes

of nanoparticles tend to be aligned even when the velocity is low (Verberne et al., 2013, 2014b), nanoparticles could ~~indirectly~~ contribute to the slip-weakening behavior. Based on these phenomena, we conclude that the mechanical weakness of brucite observed in this study is likely derived from the smooth boundary shear of fine brucite particles and alignment of the basal plane of brucite parallel to the boundary shear.

The results of several previous experimental studies showed that the friction coefficient of a mixture of strong and weak materials inversely correlates with the volume of the weak materials (Giorgetti et al., 2015; Logan and Rauenzahn, 1987; Moore and Lockner, 2011; Niemeijer and Spiers, 2007; Shimamoto and Logan, 1981; Takahashi et al., 2007; Tembe et al., 2010). Based on the maximum amount of brucite in serpentinite, that is ~20 vol. % (Kawahara et al., 2016; Moore et al., 2001), the expected friction coefficient of the antigorite–brucite mixture is 0.53, assuming a simple linear mixing law between the wet friction coefficients of 0.6 for antigorite and 0.26 for brucite. This value is not small, but the bulk friction coefficient of the mixture will decrease if weak brucite crystals are interconnected with each other. The microstructural observations showed that the shear band is less than 50 μm wide (Sect. 3.2.2; Fig. 7); therefore, a narrow network of brucite can ~~weaken~~ decrease the bulk strength. The results of a recent petrographic study of a hydrated paleo-mantle wedge revealed brucite thin films parallel to antigorite particles, suggesting the significant role of brucite in the development of the sheared structure of the antigorite–brucite assemblage in the hydrated mantle wedge (Mizukami et al., 2014). Because the maximum ~~width~~ thickness of the brucite film in the antigorite–brucite assemblage is several hundred micrometers (Kawahara et al., 2016; Mizukami et al., 2014), that is, larger than 50 μm, brucite has the potential to ~~drastically weaken the bulk strength of serpentinite~~ weaken the bulk strength of serpentinite drastically.

4.2. Application to the mantle wedge conditions

~~To interpret~~ When we consider the effect of brucite on the seismic activities in the mantle wedge, the effect of temperature should be ~~considered~~ taken into account because all our experiments were conducted under room-temperature conditions. According to previous experiments on brucite under hydrothermal conditions in which the temperature was varied, the friction coefficient and the $a - b$ values decrease with increasing temperature (Moore et al., 2001; Moore and Lockner, 2007). Because a nearly neutral $a - b$ value was observed at an effective normal stress of 150 MPa and a temperature of 340 °C (Moore et al., 2001), brucite shows ~~an~~ unstable behavior under a wide range of temperature–pressure conditions, especially at low effective normal stress. Based on the estimated frictional properties of brucite under the mantle wedge condition, we compared brucite to other mineral phases to interpret the earthquake processes within the mantle wedge (Fig. 8).

In the mantle wedge, ultramafic minerals, such as olivine, transform into serpentine minerals, such as antigorite, talc, and brucite, due to hydration. In cold subduction zones, such as beneath NE Japan, likely containing brucite under the temperature–pressure conditions of the mantle wedge, the thermodynamically stable mineral assemblages are lizardite-brucite (Liz–Brc) at depths shallower than 50 km or antigorite–brucite (Atg–Brc) assemblage under deeper and warmer conditions (Peacock and Hyndman, 1999). Previous experimental studies on antigorite suggested potential seismic activities due to the unstable frictional behavior of antigorite at high temperatures above 450 °C (Okazaki and Katayama, 2015; Takahashi et al., 2011) at which crustal (granitic) rock shows stable friction (Fig. 8), whose friction coefficient (0.5–0.7) is not as low as that of brucite (Fig. 8). Although~~,~~ lizardite, which thermodynamically destabilizes at ~200 °C, potentially shows ~~an~~ unstable frictional behavior at low temperature (Moore et al., 1997), its friction coefficient is 0.4–0.5, ~~which is~~ lower than that of antigorite but higher than that of brucite (Fig. 8). Therefore, antigorite and lizardite are not preferably deformed if other weaker minerals, such as

503 brucite, are present in continuous fault strands in which the deformation localizes. ~~Therefore, antigorite and~~
504 ~~lizardite are not preferably deformed if other weaker minerals, such as brucite, are present.~~

505 Another candidate ~~of~~ for such a weak mineral stable under mantle wedge conditions is talc. Talc
506 has a low friction coefficient of 0.1–0.2 at low to high temperatures (Fig. 8); therefore, it might contribute
507 to the creep behavior of the San Andreas fault (Moore and Lockner, 2008) or weaken the slab–mantle
508 interface (Hirauchi et al., 2013; Hyndman and Peacock, 2003). However, because talc has a stable frictional
509 behavior at any temperature, leading to aseismic creep (Moore and Lockner, 2008; Sánchez-Roa et al.,
510 2017), it cannot nucleate earthquakes. When we consider ~~Considering the occurrence of~~ talc in the mantle
511 wedge, talc is thermodynamically stable at ~~when~~ high Si concentrations and temperature. Whereas, ~~whereas~~
512 the mineral assemblage consists of brucite and antigorite when the Si content and temperature are low
513 (Peacock and Hyndman, 1999). Talc was not widely observed in the paleo-mantle wedge exposed in the
514 Shiraga body, central Shikoku, Japan, ~~with~~ at the temperature–pressure condition where the antigorite–
515 brucite system is thermodynamically stable (Kawahara et al., 2016; Mizukami et al., 2014). Although only
516 the antigorite ~~stably~~ exists stably in the antigorite–brucite stability field when the Si content is high, brucite
517 is widely distributed in the Shiraga body (~10–15 %), suggesting low Si metasomatism in the shallow
518 hydrated mantle wedge (Kawahara et al., 2016). Hence, brucite can stably exist within the mantle wedge
519 rather than talc. Although talc is still significantly important for the deformation at the subduction plate
520 interface (Hirauchi et al., 2013), the possible occurrence of brucite and its weak and unstable frictional
521 characteristics implies that brucite may be a possible control for the seismic activities at the subduction
522 plate interface in the shallow hydrated mantle wedge. ~~The distribution of brucite is associated with~~
523 ~~deformation and the brucite volume is high enough to weaken the bulk strength as discussed in Sect. 4.1;~~
524 ~~therefore, brucite might be a key mineral controlling the seismic activities in the shallow hydrated mantle~~
525 ~~wedge because brucite is the only mineral that has weak, unstable frictional characteristics under a wide~~
526 ~~range of temperature–pressure conditions (Fig. 8).~~

The results of recent seismological studies showed that ~~the~~ plate interfaces in the shallow mantle wedge have a nearly lithostatic pore pressure due to slab-derived water at various subduction zones such as SE Japan, Cascadia, Central Mexico, and Hikurangi (Audet et al., 2009; Audet and Kim, 2016; Eberhart-Phillips and Reyners, 2012; Matsubara et al., 2009; Shelly et al., 2006; Song and Kim, 2012). Such low effective normal stress conditions are conducive for brittle deformation rather than ductile behavior (French and Condit, 2019; Gao and Wang, 2017). Slow earthquakes in the mantle wedge of various subduction zones (Audet and Kim, 2016; Obara and Kato, 2016) might be induced by the low effective normal stress because the low effective normal stress conditions are conducive for the nucleation of slow earthquakes (Liu and Rice, 2007, 2009; Rubin, 2008; Segall et al., 2010). As the $a - b$ value of brucite decreases with decreasing effective normal stress, brucite at low effective normal stress possibly causes the nucleation of slow earthquakes in the mantle wedge. Notably, the possible presence of talc or brucite-free antigorite due to high Si content in the vicinity of the slab–mantle interface (Hirauchi et al., 2013; Peacock and Hyndman, 1999) might affect the partitioning of deformation (French and Condit, 2019) and the contribution of brucite to the deformation. The mechanisms of nucleation of slow earthquakes are still debated from both theoretical and experimental studies, for example, the dilatancy hardening, the transition from negative to positive $a - b$ value, the slip-weakening, or the slow stick-slip are all considered possible mechanisms (den Hartog et al., 2012; Ikari et al., 2013; Leeman et al., 2016, 2018; Matsuzawa et al., 2010; Okazaki and Katayama, 2015; Rubin, 2008; Segall et al., 2010; Shibazaki and Iio, 2003). As other serpentinite-related minerals show stable frictional behavior, i.e., positive $a - b$, friction experiments with mixtures of brucite and other minerals like talc or antigorite may provide further information on the generation of slow earthquakes. In addition, the linkage between high pore fluid pressure and the effective normal stress is still debated (Hirth and Beeler, 2015; Noda and Takahashi, 2016); therefore, experiments under hydrothermal conditions with high confining pressure and high pore fluid pressure must be conducted in the future.

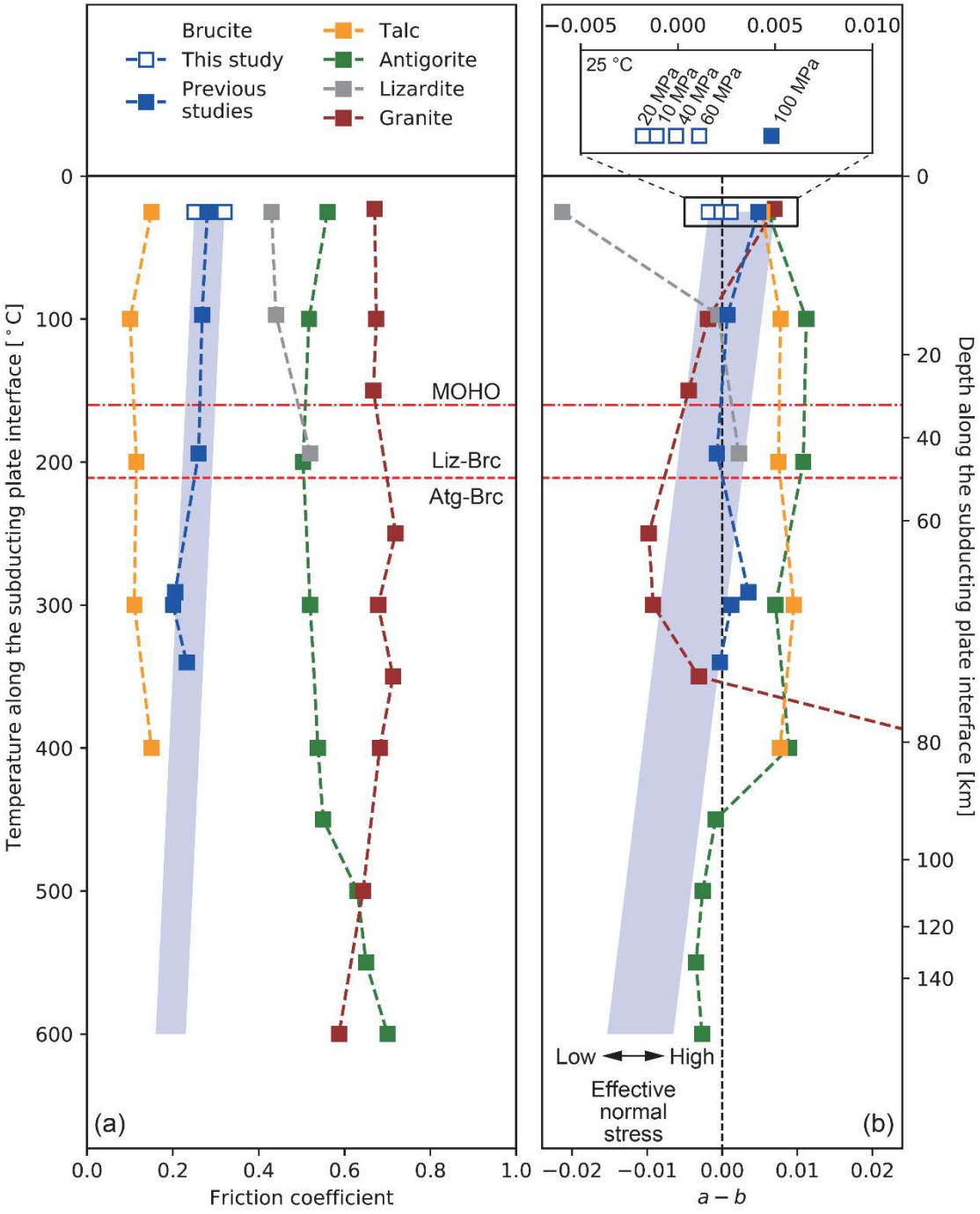

Figure 8: Friction coefficients (a) and velocity dependences (b) of brucite (this study; Moore et al., 2001), talc (Moore and Lockner, 2008), antigorite (Okazaki and Katayama, 2015; Takahashi et al., 2011), lizardite (Moore et al., 1997), and granite (Blanpied et al., 1998). The vertical axes are identical to the temperature gradient along the subduction plate interface in NE Japan (Peacock and Wang, 1999). The red chain horizontal line represents the typical depth of the MOHO. The red dotted horizontal line represents the phase boundary between lizardite–brucite (Liz–Brc) and antigorite–brucite (Atg–Brc; Peacock and Hyndman, 1999). The blue shaded areas are

the estimated frictional characteristics extrapolated from experimental results. With the decrease in the effective normal stress, the $a-b$ value decreases, as indicated by the arrow. This trend was confirmed at room temperature, as shown in the inset at the top of (b) and Fig. 4.

~~6~~5. Conclusions

In this study, the influence of effective normal stress on the frictional characteristics of brucite was experimentally determined under both dry and ~~water saturated (wet)~~ wet conditions at room temperature. The ~~steady state~~ final friction coefficients of brucite are 0.40 and 0.26 in the dry and wet cases, respectively, independently of the applied normal stress, while the peak friction coefficients are inversely correlated with the applied normal stress. In all dry experiments, velocity-weakening or stick-slip behavior was observed at every normal stress. In the wet experiments, velocity-weakening, -neutral, and -strengthening behaviors were observed at normal stresses of 10 and 20, 40, and 60 MPa, respectively. Combining with the previously reported temperature effect, this result suggests that brucite is weak and unstable under a wide range of temperature–pressure conditions. The microstructural observations reveal that the low friction coefficient and slip weakening from the peak to steady-state friction coefficient are due to the smooth boundary shear and basal plane orientation parallel to the boundary shear. Because the deformation is concentrated within a narrow shear band with a ~~width~~ thickness less than 50 μm, a small amount of brucite can weaken the bulk strength of the antigorite–brucite assemblage. Compared to other serpentinite minerals, brucite is the only mineral that shows both low friction coefficient and velocity-weakening behavior. Hence, we conclude that weak, unstable brucite contributes to the nucleation of slow earthquakes in the shallow hydrated mantle wedge.

Table 1. ***Summary of the experimental conditions and results.***

	Friction coefficient	$a-b$

Experiment	Condition	Normal stress	Final shear displacement	Peak value	Steady state (10 mm)	Steady state (20 mm)	Upsteps[a]	Downsteps[a]
HTB550	Dry	20 MPa	18 mm	0.67	0.36	0.35[b]	N/A	N/A
HTB575	Dry	20 MPa	20 mm	0.68	0.46	0.44	-0.0047±0.0003 ~~-0.0047(3)~~	-0.0048±0.0002 ~~-0.0048(2)~~
HTB580	Dry	10 MPa	20 mm	0.77	0.49	0.45	-0.0024±0.0004 ~~-0.0024(4)~~	-0.0014±0.0003 ~~-0.0014(3)~~
ND1	Dry	20 MPa	0 mm	N/A	N/A	N/A	N/A	N/A
HTB593	Dry	20 MPa	1.5 mm[c]	N/A	N/A	N/A	N/A	N/A
HTB595	Dry	20 MPa	2.0 mm[d]	0.60	N/A	N/A	N/A	N/A
HTB598	Dry	20 MPa	20 mm	0.61	0.41	0.39	-0.0010±0.0002 ~~-0.0010(2)~~	-0.0009±0.0002 ~~-0.0009(2)~~
HTB601	Dry	20 MPa	10 mm	0.65	0.42	N/A	N/A	N/A
HTB641	Dry	40 MPa	20 mm	0.51	0.41	0.395	-0.0031±0.0003[e] ~~Negative (Stick-slip)~~	-0.0020±0.0004[e] ~~Negative (Stick-slip)~~
HTB642	Dry	60 MPa	20 mm	0.50	0.40	0.39	-0.0034±0.0008[e] ~~Negative (Stick-slip)~~	-0.0012±0.0006[e] ~~Negative (Stick-slip)~~

HTB734	Wet	20 MPa	20 mm	0.35	0.28	0.25	- 0.0011±0.0002 ~~0.0011(2)~~	- 0.0018±0.0001 ~~0.0018(1)~~
HTB735	Wet	20 MPa	10 mm	0.37	0.29	N/A	N/A	N/A
HTB736	Wet	20 MPa	1.2 mm[c]	N/A	N/A	N/A	N/A	N/A
HTB737	Wet	10 MPa	20 mm	0.39	0.32	0.31	- 0.0010±0.0003 ~~0.0010(3)~~	- 0.0011±0.0002 ~~0.0011(2)~~
HTB738	Wet	20 MPa	1.8 mm[d]	0.34	N/A	N/A	N/A	N/A
HTB739	Wet	40 MPa	20 mm	0.29	0.26	0.24	0.0001±0.0002 0.0001(2)	- 0.0001±0.0001 ~~0.0001(1)~~
HTB741	Wet	60 MPa	20 mm	0.33	0.25	0.25	0.0012±0.0001 ~~0.0012(1)~~	0.0011±0.0001 ~~0.0011(1)~~

Note. [a]All parameters (a, b, and d_c) used for the velocity step tests are listed in Table S1. [b]Value at ~~the~~ a shear displacement of 18 mm. [c]Shear loading was stopped before the peak friction coefficient was reached. [d]Shear loading was stopped shortly after the peak friction coefficient was reached. [e]Stick-slip behavior was observed and $a - b$ value was determined by eq. 5.

Data availability

The results of all experimental data are available in the Supporting Information.

Author contributions

H.O. conceptualized this study. H.O. and I.K. conducted the experiments. H.O. and H.S. conducted analyses before experiments. H.O. carried out ~~the~~ formal analyses and microstructural analyses. H.O. prepared the original manuscript, which was reviewed and edited by all coauthors. K.K. was the supervisor. I.K., H.S., and K.K. designed the research project.

Competing interests

The authors declare that they have no conflict of interest.

Acknowledgement

We thank two anonymous referees for their careful and constructive reviews. We also thank Y. Noda and R. Fujioka for the experiments, H. Ishisako for the preparation of thin sections, and A. Yamaguchi and N. Ogawa for SEM observations. This research was supported by KAKENHI grants (JP20J20413, JP20H00200, JP15H02147), and the Cooperative Program (No. 114, 2019) of the Atmosphere and Ocean Research Institute, University of Tokyo. H.O. is supported by JSPS and FMSP as a research fellow.

References

Angiboust, S. and Agard, P.: Initial water budget: The key to detaching large volumes of eclogitized oceanic crust along the subduction channel?, Lithos, 120, 453–474, doi:10.1016/j.lithos.2010.09.007, 2010.

605 Anthony, J. L. and Marone, C.: Influence of particle characteristics on granular friction, J. Geophys. Res.,
606 110, B08409, doi:10.1029/2004JB003399, 2005.
607 Audet, P. and Kim, Y.: Teleseismic constraints on the geological environment of deep episodic slow
608 earthquakes in subduction zone forearcs: A review, Tectonophysics, 670, 1–15,
609 doi:10.1016/j.tecto.2016.01.005, 2016.
610 Audet, P., Bostock, M. G., Christensen, N. I. and Peacock, S. M.: Seismic evidence for overpressured
611 subducted oceanic crust and megathrust fault sealing, Nature, 457, 76–78, doi:10.1038/nature07650,
612 2009.
613 Berman, H.: Fibrous Brucite from Quebec, Am. Mineralogist, 17, 313–316, 1932.
614 Bhattacharya, P., Rubin, A. M., Bayart, E., Savage, H. M. and Marone, C.: Critical evaluation of state
615 evolution laws in rate and state friction: Fitting large velocity steps in simulated fault gouge with time-,
616 slip-, and stress-dependent constitutive laws, J. Geophys. Res. Solid Earth, 120, 6365–6385,
617 doi:10.1002/2015JB012437, 2015.
618 Bhattacharya, P., Rubin, A. M. and Beeler, N. M.: Does fault strengthening in laboratory rock friction
619 experiments really depend primarily upon time and not slip?, J. Geophys. Res. Solid Earth, 122, 6389–
620 6430, doi:10.1002/2017JB013936, 2017.
621 Blanpied, M. L., Marone, C. J., Lockner, D. A., Byerlee, J. D. and King, D. P.: Quantitative measure of
622 the variation in fault rheology due to fluid-rock interactions, J. Geophys. Res. Solid Earth, 103, 9691–
623 9712, doi:10.1029/98JB00162, 1998.
624 Bostock, M. G., Hyndman, R. D., Rondenay, S. and Peacock, S. M.: An inverted continental Moho and
625 serpentinization of the forearc mantle, Nature, 417, 536–538, doi:10.1038/417536a, 2002.
626 Calvert, A. J., Bostock, M. G., Savard, G. and Unsworth, M. J.: Cascadia low frequency earthquakes at
627 the base of an overpressured subduction shear zone, Nat. Comm., 11, 3874, doi:10.1038/s41467-020-
628 17609-3, 2020.

629 Christensen, N. I.: Serpentinites, peridotites, and seismology, Int. Geol. Rev., 46, 795–816,
630 doi:10.2747/0020-6814.46.9.795, 2004.
631 Collettini, C., Viti, C., Smith, S. A. F. and Holdsworth, R. E.: Development of interconnected talc
632 networks and weakening of continental low-angle normal faults, Geology, 37, 567–570,
633 doi:10.1130/G25645A.1, 2009.
634 D'Antonio, M. and Kristensen, M. B.: Serpentine and brucite of ultramafic clasts from the South
635 Chamorro Seamount (Ocean Drilling Program Leg 195, Site 1200): inferences for the serpentinization of
636 the Mariana forearc mantle, Mineral. Mag., 68, 887–904, doi:10.1180/0026461046860229, 2004.
637 Deer, W. A., Howie, R. A. and Zussman, J.: An introduction to the rock-forming minerals, 3rd edition,
638 The Mineralogical Society, London, United Kingdom, 2013.
639 den Hartog, S. A. M. and Spiers, C. J.: A microphysical model for fault gouge friction applied to
640 subduction megathrusts, J. Geophys. Res. Solid Earth, 119, 1510–1529, doi:10.1002/2013JB010580,
641 2014.
642 den Hartog, S. A. M., Peach, C. J., de Winter, D. A. M., Spiers, C. J. and Shimamoto, T.: Frictional
643 properties of megathrust fault gouges at low sliding velocities: New data on effects of normal stress and
644 temperature, J. Struct. Geol., 38, 156–171, doi:10.1016/j.jsg.2011.12.001, 2012.
645 DeShon, H. R. and Schwartz, S. Y.: Evidence for serpentinization of the forearc mantle wedge along the
646 Nicoya Peninsula, Costa Rica, Geophys. Res. Lett., 31, L21611, doi:10.1029/2004GL021179, 2004.
647 Dieterich, J. H.: Modeling of rock friction: 1. Experimental results and constitutive equations, J. Geophys.
648 Res., 84, 2161, doi:10.1029/JB084iB05p02161, 1979.
649 Dorbath, C., Gerbault, M., Carlier, G. and Guiraud, M.: Double seismic zone of the Nazca plate in
650 northern Chile: High-resolution velocity structure, petrological implications, and thermomechanical
651 modeling, Geochem. Geophys. Geosyst., 9, Q07006, doi:10.1029/2008GC002020, 2008.

652 Eberhart-Phillips, D. and Reyners, M.: Imaging the Hikurangi Plate interface region, with improved local-
653 earthquake tomography, Geophys. J. Int., 190, 1221–1242, doi:10.1111/j.1365-246X.2012.05553.x, 2012.
654 Evans, B. W., Hattori, K. and Baronnet, A.: Serpentinite: what, why, where?, Elements, 9, 99–106,
655 doi:10.2113/gselements.9.2.99, 2013.
656 Fagereng, Å. and den Hartog, S. A. M.: Subduction megathrust creep governed by pressure solution and
657 frictional–viscous flow, Nat. Geosci., 10, 51–57, doi:10.1038/ngeo2857, 2017.
658 French, M. E. and Condit, C. B.: Slip partitioning along an idealized subduction plate boundary at deep
659 slow slip conditions, Earth Planet. Sci. Lett., 528, 115828, doi:10.1016/j.epsl.2019.115828, 2019.
660 Gao, X. and Wang, K.: Rheological separation of the megathrust seismogenic zone and episodic tremor
661 and slip, Nature, 543, 416–419, doi:10.1038/nature21389, 2017.
662 Giorgetti, C., Carpenter, B. M. and Collettini, C.: Frictional behavior of talc-calcite mixtures, J. Geophys.
663 Res. Solid Earth, 120, 6614–6633, doi:10.1002/2015JB011970, 2015.
664 Guillot, S. and Hattori, K.: Serpentinites: essential roles in geodynamics, arc volcanism, sustainable
665 development, and the origin of life, Elements, 9, 95–98, doi:10.2113/gselements.9.2.95, 2013.
666 Guillot, S., Hattori, K., Agard, P., Schwartz, S. and Vidal, O.: Exhumation processes in oceanic and
667 continental subduction conetxts: a review, in: Subduction zone geodynamics, edited by S. Lallemand and
668 F. Funiciello, Springer, Berlin, Heidelberg, Germany, 175–205, 2009.
669 Guillot, S., Schwartz, S., Reynard, B., Agard, P. and Prigent, C.: Tectonic significance of serpentinites,
670 Tectonophysics, 646, 1–19, doi:10.1016/j.tecto.2015.01.020, 2015.
671 Haines, S. H., Kaproth, B., Marone, C., Saffer, D. M. and van der Pluijm, B. A.: Shear zones in clay-rich
672 fault gouge: A laboratory study of fabric development and evolution, J. Struct. Geol., 51, 206–225,
673 doi:10.1016/j.jsg.2013.01.002, 2013.
674 Hirauchi, K., den Hartog, S. A. M. and Spiers, C. J.: Weakening of the slab–mantle wedge interface
675 induced by metasomatic growth of talc, Geology, 41, 75–78, doi:10.1130/G33552.1, 2013.

676 Hirth, G. and Beeler, N. M.: The role of fluid pressure on frictional behavior at the base of the
677 seismogenic zone, Geology, 43, 223–226, doi:10.1130/G36361.1, 2015.
678 Hirth, G. and Guillot, S.: Rheology and tectonic significance of serpentinite, Elements, 9, 107–113,
679 doi:10.2113/gselements.9.2.107, 2013.
680 Horn, H. M. and Deere, D. U.: Frictional characteristics of minerals, Géotechnique, 12, 319–335,
681 doi:10.1680/geot.1962.12.4.319, 1962.
682 Hostetler, P. B., Coleman, R. G., Mumpton, F. A. and Evans, B. W.: Brucite in alpine serpentinites, Am.
683 Mineralogist, 51, 75–98, 1966.
684 Hyndman, R. D. and Peacock, S. M.: Serpentinization of the forearc mantle, Earth Planet. Sci. Lett., 212,
685 417–432, doi:10.1016/S0012-821X(03)00263-2, 2003.
686 Ide, S., Beroza, G. C., Shelly, D. R. and Uchide, T.: A scaling law for slow earthquakes, Nature, 447, 76–
687 79, doi:10.1038/nature05780, 2007.
688 Ikari, M. J., Marone, C., Saffer, D. M. and Kopf, A. J.: Slip weakening as a mechanism for slow
689 earthquakes, Nat. Geosci., 6, 468–472, doi:10.1038/ngeo1818, 2013.
690 Kawahara, H., Endo, S., Wallis, S. R., Nagaya, T., Mori, H. and Asahara, Y.: Brucite as an important
691 phase of the shallow mantle wedge: Evidence from the Shiraga unit of the Sanbagawa subduction zone,
692 SW Japan, Lithos, 254–255, 53–66, doi:10.1016/j.lithos.2016.02.022, 2016.
693 Kawai, K., Sakuma, H., Katayama, I. and Tamura, K.: Frictional characteristics of single and
694 polycrystalline muscovite and influence of fluid chemistry, J. Geophys. Res. Solid Earth, 120, 6209–
695 6218, doi:10.1002/2015JB012286, 2015.
696 Kawakatsu, H. and Watada, S.: Seismic evidence for deep-water transportation in the mantle, Science,
697 316, 1468–1471, doi:10.1126/science.1140855, 2007.

698 Kenigsberg, A. R., Rivière, J., Marone, C. and Saffer, D. M.: The effects of shear strain, fabric, and
699 porosity evolution on elastic and mechanical properties of clay-rich fault gouge, J. Geophys. Res. Solid
700 Earth, 10968-10982, doi:10.1029/2019JB017944, 2019.
701 Kenigsberg, A. R., Rivière, J., Marone, C. and Saffer, D. M.: Evolution of elastic and mechanical
702 properties during fault shear: The roles of clay content, fabric development, and porosity, J. Geophys.
703 Res. Solid Earth, 125, e2019JB018612, doi:10.1029/2019JB018612, 2020.
704 Leeman, J. R., Saffer, D. M., Scuderi, M. M. and Marone, C.: Laboratory observations of slow
705 earthquakes and the spectrum of tectonic fault slip modes, Nat. Comm., 7, 11104,
706 doi:10.1038/ncomms11104, 2016.
707 Leeman, J. R., Marone, C. and Saffer, D. M.: Frictional mechanics of slow earthquakes, J. Geophys. Res.
708 Solid Earth, 123, 7931–7949, doi:10.1029/2018JB015768, 2018.
709 Liu, Y. and Rice, J. R.: Spontaneous and triggered aseismic deformation transients in a subduction fault
710 model, J. Geophys. Res., 112, B09404, doi:10.1029/2007JB004930, 2007.
711 Liu, Y. and Rice, J. R.: Slow slip predictions based on granite and gabbro friction data compared to GPS
712 measurements in northern Cascadia, J. Geophys. Res. Solid Earth, 114, 1–19,
713 doi:10.1029/2008JB006142, 2009.
714 Logan, J. M. and Rauenzahn, K. A.: Frictional dependence of gouge mixtures of quartz and
715 montmorillonite on velocity, composition and fabric, Tectonophysics, 144, 87–108, doi:10.1016/0040-
716 1951(87)90010-2, 1987.
717 Logan, J. M., Dengo, C. A., Higgs, N. G. and Wang, Z. Z.: Fabrics of experimental fault zones: Their
718 development and eelationship to mechanical behavior, in: Fault Mechanics and Transport Properties of
719 Rocks, edited by Evans, B, and Wong, T.F., Elsevier, 33–67, 1992.

720 Manning, C. E.: Coupled reaction and flow in subduction zones: Silica metasomatism in the mantle
721 wedge, in: Fluid Flow and Transport in Rocks, edited by Jamtveit, B., and Yardley, B.W.D., Springer,
722 Dordrecht, the Netherlands, 139–148, 1997.
723 Marone, C.: Laboratory-derived friction laws and their application to seismic faulting, Annu. Rev. Earth
724 Planet. Sci., 26, 643–696, doi:10.1146/annurev.earth.26.1.643, 1998.
725 Marone, C. and Kilgore, B. D.: Scaling of the critical slip distance for seismic faulting with shear strain in
726 fault zones, Nature, 362, 618–621, doi:10.1038/362618a0, 1993.
727 Matsubara, M., Obara, K. and Kasahara, K.: High-VP/VS zone accompanying non-volcanic tremors and
728 slow-slip events beneath southwestern Japan, Tectonophysics, 472, 6–17,
729 doi:10.1016/j.tecto.2008.06.013, 2009.
730 Matsuzawa, T., Hirose, H., Shibazaki, B. and Obara, K.: Modeling short- and long-term slow slip events
731 in the seismic cycles of large subduction earthquakes, J. Geophys. Res., 115, B12301,
732 doi:10.1029/2010JB007566, 2010.
733 Mizukami, T., Yokoyama, H., Hiramatsu, Y., Arai, S., Kawahara, H., Nagaya, T. and Wallis, S. R.: Two
734 types of antigorite serpentinite controlling heterogeneous slow-slip behaviours of slab–mantle interface,
735 Earth Planet. Sci. Lett., 401, 148–158, doi:10.1016/j.epsl.2014.06.009, 2014.
736 Moore, D. E. and Lockner, D. A.: Crystallographic controls on the frictional behavior of dry and water-
737 saturated sheet structure minerals, J. Geophys. Res., 109, B03401, doi:10.1029/2003JB002582, 2004.
738 Moore, D. E. and Lockner, D. A.: Comparative deformation behavior of minerals in serpentinized
739 ultramafic rock: Application to the slab-mantle interface in subduction zones, Int. Geol. Rev., 49, 401–
740 415, doi:10.2747/0020-6814.49.5.401, 2007.
741 Moore, D. E. and Lockner, D. A.: Talc friction in the temperature range 25°–400 °C: Relevance for fault-
742 zone weakening, Tectonophysics, 449, 120–132, doi:10.1016/j.tecto.2007.11.039, 2008.

743 Moore, D. E. and Lockner, D. A.: Frictional strengths of talc-serpentine and talc-quartz mixtures, J.
744 Geophys. Res., 116, B01403, doi:10.1029/2010JB007881, 2011.
745 Moore, D. E., Lockner, D. A., Ma, S., Summers, R. and Byerlee, J. D.: Strengths of serpentinite gouges at
746 elevated temperatures, J. Geophys. Res. Solid Earth, 102, 14787–14801, doi:10.1029/97JB00995, 1997.
747 Moore, D. E., Lockner, D. A., Iwata, K., Tanaka, H. and Byerlee, J. D.: How brucite may affect the
748 frictional properties of serpentinite, USGS Open-File Report, 1–14, 2001.
749 Morrow, C. A., Moore, D. E. and Lockner, D. A.: The effect of mineral bond strength and adsorbed water
750 on fault gouge frictional strength, Geophys. Res. Lett., 27, 815–818, doi:10.1029/1999GL008401, 2000.
751 Nagaya, T., Okamoto, A., Oyanagi, R., Seto, Y., Miyake, A., Uno, M., Muto, J. and Wallis, S. R.:
752 Crystallographic preferred orientation of talc determined by an improved EBSD procedure for sheet
753 silicates: Implications for anisotropy at the slab–mantle interface due to Si-metasomatism, Am.
754 Mineralogist, 105, 873–893, doi:10.2138/am-2020-7006, 2020.
755 Nakajima, J., Tsuji, Y., Hasegawa, A., Kita, S., Okada, T. and Matsuzawa, T.: Tomographic imaging of
756 hydrated crust and mantle in the subducting Pacific slab beneath Hokkaido, Japan: Evidence for
757 dehydration embrittlement as a cause of intraslab earthquakes, Gondwana Res., 16, 470–481,
758 doi:10.1016/j.gr.2008.12.010, 2009.
759 Niemeijer, A. R.: Velocity-dependent slip weakening by the combined operation of pressure solution and
760 foliation development, Sci. Rep., 8, 4724, doi:10.1038/s41598-018-22889-3, 2018.
761 Niemeijer, A. R. and Spiers, C. J.: A microphysical model for strong velocity weakening in phyllosilicate-
762 bearing fault gouges, J. Geophys. Res., 112, B10405, doi:10.1029/2007JB005008, 2007.
763 Noda, H. and Shimamoto, T.: Constitutive properties of clayey fault gouge from the Hanaore fault zone,
764 southwest Japan, J. Geophys. Res., 114, B04409, doi:10.1029/2008JB005683, 2009.
765 Noda, H. and Takahashi, M.: The effective stress law at a brittle-plastic transition with a halite gouge
766 layer, Geophys. Res. Lett., 43, 1966–1972, doi:10.1002/2015GL067544, 2016.

767 Obara, K.: Nonvolcanic Deep Tremor Associated with Subduction in Southwest Japan, Science, 296,
768 1679–1681, doi:10.1126/science.1070378, 2002.
769 Obara, K. and Kato, A.: Connecting slow earthquakes to huge earthquakes, Science, 353, 253–257,
770 doi:10.1126/science.aaf1512, 2016.
771 Okamoto, A. S., Verberne, B. A., Niemeijer, A. R., Takahashi, M., Shimizu, I., Ueda, T. and Spiers, C. J.:
772 Frictional properties of simulated chlorite gouge at hydrothermal conditions: Implications for subduction
773 megathrusts, J. Geophys. Res. Solid Earth, 124, 4545–4565, doi:10.1029/2018JB017205, 2019.
774 Okazaki, K. and Katayama, I.: Slow stick slip of antigorite serpentinite under hydrothermal conditions as
775 a possible mechanism for slow earthquakes, Geophys. Res. Lett., 42, 1099–1104,
776 doi:10.1002/2014GL062735, 2015.
777 Okuda, H., Kawai, K. and Sakuma, H.: First-principles investigation of frictional characteristics of
778 brucite: An application to its macroscopic frictional characteristics, J. Geophys. Res. Solid Earth, 124,
779 10423–10443, doi:10.1029/2019JB017740, 2019.
780 Oleskevich, D. A., Hyndman, R. D. and Wang, K.: The updip and downdip limits to great subduction
781 earthquakes: Thermal and structural models of Cascadia, south Alaska, SW Japan, and Chile, J. Geophys.
782 Res. Solid Earth, 104, 14965–14991, doi:10.1029/1999JB900060, 1999.
783 Oyanagi, R., Okamoto, A., Hirano, N. and Tsuchiya, N.: Competitive hydration and dehydration at
784 olivine–quartz boundary revealed by hydrothermal experiments: Implications for silica metasomatism at
785 the crust–mantle boundary, Earth Planet. Sci. Lett., 425, 44–54, doi:10.1016/j.epsl.2015.05.046, 2015.
786 Oyanagi, R., Okamoto, A. and Tsuchiya, N.: Silica controls on hydration kinetics during serpentinization
787 of olivine: Insights from hydrothermal experiments and a reactive transport model, Geochim.
788 Cosmochim. Acta, 270, 21–42, doi:10.1016/j.gca.2019.11.017, 2020.
789 Peacock, S. M. and Hyndman, R. D.: Hydrous minerals in the mantle wedge and the maximum depth of
790 subduction thrust earthquakes, Geophys. Res. Lett., 26, 2517–2520, doi:10.1029/1999GL900558, 1999.

791 Peacock, S. M. and Wang, K.: Seismic consequences of warm versus cool subduction metamorphism:
792 Examples from southwest and northeast Japan, Science, 286, 937–939,
793 doi:10.1126/science.286.5441.937, 1999.
794 Ramachandran, K. and Hyndman, R. D.: The fate of fluids released from subducting slab in northern
795 Cascadia, Solid Earth, 3, 121–129, doi:10.5194/se-3-121-2012, 2012.
796 Reinen, L. A., Weeks, J. D. and Tullis, T. E.: The frictional behavior of lizardite and antigorite
797 serpentinites: Experiments, constitutive models, and implications for natural faults, Pure Appl. Geophys.,
798 143, 317–358, doi:10.1007/BF00874334, 1994.
799 Reynard, B.: Serpentine in active subduction zones, Lithos, 178, 171–185,
800 doi:10.1016/j.lithos.2012.10.012, 2013.
801 Rogers, G. and Dragert, H.: Episodic tremor and slip on the cascadia subduction zone: The chatter of
802 silent slip, Science, 300, 1942–1943, doi:10.1126/science.1084783, 2003.
803 Rubin, A. M.: Episodic slow slip events and rate-and-state friction, J. Geophys. Res., 113, B11414,
804 doi:10.1029/2008JB005642, 2008.
805 Rubinstein, J. L., Vidale, J. E., Gomberg, J., Bodin, P., Creager, K. C. and Malone, S. D.: Non-volcanic
806 tremor driven by large transient shear stresses, Nature, 448, 579–582, doi:10.1038/nature06017, 2007.
807 Rubinstein, J. L., La Rocca, M., Vidale, J. E., Creager, K. C. and Wech, A. G.: Tidal modulation of
808 nonvolcanic tremor, Science, 319, 186–189, doi:10.1126/science.1150558, 2008.
809 Ruina, A. L.: Slip instability and state variable friction laws, J. Geophys. Res. Solid Earth, 88, 10359–
810 10370, doi:10.1029/JB088iB12p10359, 1983.
811 Sánchez-Roa, C., Faulkner, D. R., Boulton, C., Jimenez-Millan, J. and Nieto, F.: How phyllosilicate
812 mineral structure affects fault strength in Mg-rich fault systems, Geophys.Res. Lett., 44, 5457–5467,
813 doi:10.1002/2017GL073055, 2017.

814 Schmidt, D. A. and Gao, H.: Source parameters and time-dependent slip distributions of slow slip events
815 on the Cascadia subduction zone from 1998 to 2008, J. Geophys. Res., 115, B00A18,
816 doi:10.1029/2008JB006045, 2010.
817 Segall, P., Rubin, A. M., Bradley, A. M. and Rice, J. R.: Dilatant strengthening as a mechanism for slow
818 slip events, J. Geophys. Res., 115, B12305, doi:10.1029/2010JB007449, 2010.
819 Shelly, D. R., Beroza, G. C., Ide, S. and Nakamula, S.: Low-frequency earthquakes in Shikoku, Japan,
820 and their relationship to episodic tremor and slip, Nature, 442, 188–191, doi:10.1038/nature04931, 2006.
821 Shibazaki, B. and Iio, Y.: On the physical mechanism of silent slip events along the deeper part of the
822 seismogenic zone, Geophys. Res. Lett., 30, 1489, doi:10.1029/2003GL017047, 2003.
823 Shimamoto, T. and Logan, J. M.: Effects of simulated clay gouges on the sliding behavior of Tennessee
824 sandstone, Tectonophysics, 75, 243–255, doi:10.1016/0040-1951(81)90276-6, 1981.
825 Siman-Tov, S., Aharonov, E., Sagy, A. and Emmanuel, S.: Nanograins form carbonate fault mirrors,
826 Geology, 41, 703–706, doi:10.1130/G34087.1, 2013.
827 Skarbek, R. M. and Savage, H. M.: RSFit3000: A MATLAB GUI-based program for determining rate
828 and state frictional parameters from experimental data, Geosphere, 15, 1665–1676,
829 doi:10.1130/GES02122.1, 2019.
830 Song, T.-R. A. and Kim, Y.: Localized seismic anisotropy associated with long-term slow-slip events
831 beneath southern Mexico, Geophys. Res. Lett., 39, L09308, doi:10.1029/2012GL051324, 2012.
832 Takahashi, M., Mizoguchi, K., Kitamura, K. and Masuda, K.: Effects of clay content on the frictional
833 strength and fluid transport property of faults, J. Geophys. Res., 112, B08206,
834 doi:10.1029/2006JB004678, 2007.
835 Takahashi, M., Uehara, S.-I., Mizoguchi, K., Shimizu, I., Okazaki, K. and Masuda, K.: On the transient
836 response of serpentine (antigorite) gouge to stepwise changes in slip velocity under high-temperature
837 conditions, J. Geophys. Res., 116, B10405, doi:10.1029/2010JB008062, 2011.

838 Tarling, M. S., Smith, S. A. F. and Scott, J. M.: Fluid overpressure from chemical reactions in serpentinite
839 within the source region of deep episodic tremor, Nat. Geosci., 12, 1034–1042, doi:10.1038/s41561-019-
840 0470-z, 2019.
841 Tembe, S., Lockner, D. A. and Wong, T.-F.: Effect of clay content and mineralogy on frictional sliding
842 behavior of simulated gouges: Binary and ternary mixtures of quartz, illite, and montmorillonite, J.
843 Geophys. Res., 115, B03416, doi:10.1029/2009JB006383, 2010.
844 Tesei, T., Harbord, C. W. A., De Paola, N., Collettini, C. and Viti, C.: Friction of mineralogically
845 controlled serpentinites and implications for fault weakness, J. Geophys. Res. Solid Earth, 123, 6976–
846 6991, doi:10.1029/2018JB016058, 2018.
847 Verberne, B. A., De Bresser, J. H. P., Niemeijer, A. R., Spiers, C. J., de Winter, D. A. M. and Plümper,
848 O.: Nanocrystalline slip zones in calcite fault gouge show intense crystallographic preferred orientation:
849 Crystal plasticity at sub-seismic slip rates at 18–150 °C, Geology, 41, 863–866, doi:10.1130/G34279.1,
850 2013.
851 Verberne, B. A., Spiers, C. J., Niemeijer, A. R., De Bresser, J. H. P., de Winter, D. A. M. and Plümper,
852 O.: Frictional properties and microstructure of calcite-rich fault gouges sheared at sub-seismic sliding
853 velocities, Pure Appl. Geophys., 171, 2617–2640, doi:10.1007/s00024-013-0760-0, 2014a.
854 Verberne, B. A., Plümper, O., de Winter, D. A. M. and Spiers, C. J.: Superplastic nanofibrous slip zones
855 control seismogenic fault friction, Science, 346, 1342–1344, doi:10.1126/science.1259003, 2014b.
856 Viti, C.: Exploring fault rocks at the nanoscale, J. Struct. Geol., 33, 1715–1727,
857 doi:10.1016/j.jsg.2011.10.005, 2011.
858